Pan-Arctic Ocean primary production constrained by turbulent nitrate fluxes

Achim Randelhoff[1,2]*, **Johnna Holding**[3,4], **Markus Janout**[5], **Mikael Kristian Sejr**[3,4], **Jean-Éric Tremblay**[1,2], **Matthew B. Alkire**[6,7]

[1] Takuvik Joint International Laboratory, Université Laval (QC, Canada) and CNRS (France)

[2] Département de biologie and Québec-Océan, Université Laval (QC, Canada)

[3] Arctic Research Centre, Aarhus University, Ny Munkegade 114, bldg. 1540, 8000 Aarhus C, Denmark

[4] Department of Bioscience, Aarhus University, Vejlsøvej 25, 8600, Silkeborg, Denmark

[5] Alfred-Wegener-Institute Helmholtz Center for Polar and Marine Research, Am Handelshafen 12, D-27570 Bremerhaven, Germany

[6] Applied Physics Laboratory, University of Washington, Seattle, WA USA

[7] Now at: School of Oceanography, University of Washington, Seattle, WA USA

* **Correspondance**:

Achim Randelhoff, achim.randelhoff@takuvik.ulaval.ca

Keywords: Arctic, turbulence, nitrate, flux, primary production, climate change, sea ice

Abstract

Arctic Ocean primary productivity is limited by light and inorganic nutrients. With recent decades' decreasing sea ice cover, nitrate limitation is thought to become more prominent. Although much has been learned about nitrate supply from general patterns of ocean circulation and water column stability, a quantitative analysis requires dedicated turbulence measurements that have only started to accumulate in the last dozen years. Here we present new observations of the turbulent vertical nitrate flux in the Laptev Sea, Baffin Bay, and Young Sound (North-East

Greenland), supplemented by a compilation of 13 published estimates throughout the Arctic Ocean. Combining those with a Pan-Arctic database of in situ measurements of nitrate concentration and density, we found the annual nitrate inventory to be largely determined by the strength of stratification, but also by bathymetry. Nitrate fluxes explained the observed regional patterns and magnitudes of both new primary production and particle export. We argue that with few regional exceptions, vertical turbulent nitrate fluxes are a reliable proxy of Arctic primary production accessible by autonomous and large-scale measurements. They also provide a framework to project nutrient limitation scenarios into the future based on clear energetic and mass budget constraints resulting from turbulent mixing and freshwater flows.

1 Introduction

Without upward mixing of nutrients, much of the ocean would harbour no life (Ambühl, 1959; Margalef, 1978); the Arctic Ocean is no exception. The reason is essentially that algae, in particular dead algae, and other particulate matter have the tendency to sink due to their higher density, and hence nutrients are constantly being removed from the surface waters. Phytoplankton, in turn, has to rely on a resupply of nutrients in order to be able to grow and re-build their standing stock every year. Consequently, primary production, which occurs in the euphotic zone where light levels are sufficient to support net growth, depends on how much new nitrate is brought up from below the photic zone each year and is hence available to new production (see Appendix and Dugdale and Goering, 1967).

While turbulence is a concern for aquatic life everywhere, the Arctic Ocean is special in certain regards, most notably its ubiquitous sea ice cover and the strong stratification linked to its estuarine nature (Aagaard and Carmack, 1989). Large summertime accumulation of meltwater from sea ice and terrestrial runoff has profound impacts on the vertical mixing in the upper ocean (Cole et al., 2018; McPhee and Kantha, 1989; Randelhoff et al., 2017). The Arctic seasonal freeze-melt alternation dominates over diurnal cycles (McPhee, 1992) due to low sun angles, such that there is often only seasonal nitrate limitation, and winter mixing is disproportionately important for setting mixed-layer properties, as will be shown throughout this paper.

Sea ice is often assumed to be a rather rigid lid that shuts out a large portion of the sunlight as well as wind energy that could otherwise mix the ocean. As much of this ice is melting in the course of the 21st century (Comiso, 2012), the factors limiting Arctic marine growth will likely change. Such a transition in limiting factors usually leads to difficulties in predicting systems (Allen and Hoekstra, 2015). Indeed, Vancoppenolle et al. (2013) found that three different coupled biogeochemical general circulation models and their predictions for integrated Arctic Ocean primary production until the end of this century show vastly diverging trajectories beyond a few decades from now. In their analysis, a prominent uncertainty concerned the resupply of nitrate to the photic zone, which is currently not well constrained. Hence one practical implication of our lack of understanding of the vertical nitrate flux is the failure to consistently predict future Arctic Ocean primary production.

Stratification inhibits vertical mixing (Osborn, 1980) and hence turbulent nitrate fluxes. The Arctic Ocean can furthermore be divided into a weakly stratified Atlantic sector and a strongly stratified Pacific one (e.g. Carmack, 2007; Bluhm et al., 2015; Tremblay et al., 2015). Vertical turbulent nitrate fluxes are hence routinely invoked to explain patterns of primary production across the Arctic, such as basin scale differences (Carmack et al., 2006; Randelhoff and Guthrie, 2016; Tremblay et al., 2015), but also an apparently increasing prevalence of fall blooms (Ardyna et al., 2014; Nishino et al., 2015), and even fjord scale differences depending on glacier morphology (Hopwood et al., 2018). These observations are mostly qualitative and rarely quantified with direct measurements. Whereas the vertical nitrate flux in the world ocean has received attention at least since the late 1980s (Lewis et al., 1986), dedicated measurements in the Arctic Ocean have only started to accumulate in the last dozen years. We use this opportunity to summarize the current state of knowledge, test critical hypotheses about Arctic marine productivity, and outline further research directions to unify physical constraints of Arctic Ocean primary production.

Physical processes other than vertical mixing, such as advection (Torres-Valdés et al., 2013), upwelling (Carmack and Chapman, 2003; Randelhoff and Sundfjord, 2018), or mesoscale horizontal mixing through eddies (Watanabe et al., 2014), may also play a role at least regionally, but will turn out to be unnecessary to invoke in order to explain Arctic Ocean productivity within the scope of this paper. We will hence neglect those processes for the time being and discuss them in more detail after the Conclusions.

2 Material & methods

This study is centered around a compilation of measurements and estimates of the upward vertical turbulent flux of nitrate in different locations across the Arctic Ocean. In this study, we present 4 new measurements and estimates, along with a dozen values already published. We further supplemented the nitrate fluxes with a collection of vertical profiles of seawater nitrate concentration.

2.1 Compilation of NO_3^- concentrations

The Pan-Arctic data base carefully compiled by Codispoti et al. (2013) was downloaded from the NOAA website under NODC accession number 0072133. An additional database covered the Canadian Archipelago using various ArcticNet and Fisheries and Oceans Canada cruises, compiled by Coupel et al. (2019, in prep.). We included more winter data, notoriously scarce in the Arctic, by downloading data from the Chukchi shelf as presented by Arrigo et al. (2017). For each profile, we derived (1) the Brunt-Väisälä buoyancy frequency in the depth interval from 30 to 60 m as an indicator of the strength of stratification and (2) the surface nitrate concentration.

2.2 Nitrate flux compilation

In order to compile previously published estimates of vertical turbulent nitrate fluxes in the Arctic Ocean, we relied mostly on our knowledge of the literature, given the small amount of relevant publications. Additionally, we performed a search on Web of Science using the search term `TS=((nitr* AND suppl*) OR (nitr* AND flux*) OR (nitr* AND mix*)) AND TS=((Arctic OR Polar) AND Ocean) AND TS=(vertical OR turbulen*) AND WC=Ocean*`, which resulted in 95 publications that were individually screened for relevance. We only included measurements and estimates based on in-situ observations.

The resulting list comprised just above a dozen flux estimates going back to less than ten publications. To improve data coverage, we had conducted a number of additional field expeditions and evaluated existing data opportunistically. In this study, we present new measurements from the Laptev Sea, Baffin Bay, and Young Sound, as well as a re-calculation of published observations from the Chukchi Sea (Nishino et al., 2015). In order to not disrupt the flow of the main text, details of the respective methods and field campaigns are deferred to the Appendix.

Briefly, our three-week-long summer sampling campaign in Young Sound (a North East Greenland fjord) sought to quantify turbulent mixing, vertical nitrate supply, and new (nitrate-based) production in a fjord strongly affected by meltwater from the Greenland Ice Sheet. From the Laptev Sea, we present a small selection of representative vertical profiles of nitrate concentrations and oceanic microstructure, collected in the years 2008-2018. From Baffin Bay, we made use of a novel year-long 2017-18 time series of autonomous profilers, so-called biogeochemical (BGC) Argo floats (Biogeochemical-Argo Planning Group, 2016). These were specially adapted in order to function under the ice cover lasting from November to July. Based on the evolution of the upper-ocean nitrate inventory, we inferred the part due to vertical mixing. We further used a data set of nitrate concentrations and turbulent microstructure in the Chukchi Sea (Nishino et al., 2015) to calculate another estimate of vertical nitrate fluxes during early fall.

For the majority of those experiments, turbulence (microstructure) data were measured; just as was the case for the literature values. In some cases, turbulent mixing was inferred from current finestructure; see also the Appendix. Nitrate fluxes were generally calculated across the nitracline, meaning by combining a nitracline-average turbulent diffusivity with the strength of the nitrate gradient. Individual methodologies may however vary regarding e.g. choice of vertical layer or averaging procedures. According to our personal experience, such choices may make a difference for individual calculations, but less so for large-scale averages, and hence we take the fluxes recorded in the literature at face value. A systematic assessment of potential methodological errors has to our knowledge however not been conducted.

For a more detailed discussion of how vertical nitrate fluxes are measured, see the Appendix.

For each of the estimates of the vertical turbulent nitrate flux, we also extracted the end-of-winter surface nitrate concentration either from the same publication or from related studies. The specific references are given in the supplementary material. Our entire data set is presented in Table 1; note that it mixes vertical nitrate fluxes across different seasons, vertical levels, regions, and sample sizes.

2.3 Comparison between nitrate fluxes and primary production

We compared nitrate fluxes with new production (primary production based on assimilation of nitrate, see Dugdale and Goering (1967)) and export production. New production estimates were taken from Sakshaug (2004). Export production estimates were taken from Wiedmann (2015), who has compiled the vertical carbon export flux at 200 m depth. To enhance data coverage, we added to this compilation measurements from two studies from the Central Arctic Ocean (Cai et al., 2010; Honjo et al., 2010). Details can be found in the Supplementary Material

Both biomass and primary production are frequently given in units of carbon. To convert between units of carbon and nitrate fluxes, we employed a C:N ratio of 6.6 mol C: mol N, the so-called Redfield ratio (Redfield et al., 1963). This particular choice of C:N ratio may be criticized on the grounds that they vary depending on the type of organic matter and other environmental factors (Brzezinski, 1985; Tamelander et al., 2013), and that C:N ratios observed in the Arctic in particular are usually higher (Frigstad et al., 2014). However, turbulence measurements usually come with a much larger margin of error, with one detailed study giving the systematic bias between two different sets of microstructure probes, signal processing, and calibration procedures as within a factor of 2 (Moum et al., 1995). This is impressive for microstructure measurements but significantly larger than the accuracy with which the C:N ratio is frequently discussed in biogeochemical contexts. Therefore, by assuming a standard, constant C:N ratio, we make our results easy to adapt to other ratios should the reader want to change this number.

3 Results

3.1 Seasonal cycle of surface nitrate concentration

Winter surface nitrate concentrations in the Atlantic sector reached high values around 11 µM (Fig. 1). In the Central Arctic Ocean, concentrations stayed constant at roughly 1-3 µM throughout the year, whereas in the coastal Beaufort Sea they occasionally reached intermediate values in winter. Most regions of the Arctic however become nitrate limited (<1µM) during the summer, with the exception of the Eurasian Basin, the Makarov Basin, and some regions in Southern Fram Strait.

3.2 Nitrate fluxes

Nitrate flux estimates are still scarce given that they require co-located measurements of both turbulence and nitrate concentrations; however, they slowly approach Pan-Arctic coverage (Fig. 2). Highest values (> 1 mmol N m^{-2} d^{-1}) were found in the Atlantic sector. The lowest values (<< 0.1 mmol N m^{-2} d^{-1}) occurred in the central basins (Canada Basin) and in Young Sound and the Laptev Sea, two locations strongly impacted by terrestrial freshwater.

3.3 Nitrate flux seasonality

The seasonal cycle of surface nitrate concentration was also reflected in its upward fluxes (Fig. 3). In areas where the water column overturned in summer, summer fluxes were an order of magnitude below winter values. A notable exception seemed to be one station in the Barents Sea south of the polar front (Wiedmann et al., 2017), where the water was weakly stratified even in summer and hence nitrate fluxes were probably at least as high as in winter with 5 mmol N m^{-2} d^{-1} (Table 1), although sample size (N=1) was not sufficient to draw further conclusions.

Observations over a full seasonal cycle were only available in areas where the water column overturns, notable due to measurements from the Barents sea and shelf slope area (Table 1). In contrast, in the non-overturning regions, fluxes were lower overall, but there is not enough data to test whether the seasonality itself is, in relative terms, really much weaker there.

4 Discussion

4.1 Nitrate fluxes as a function of stratification and seasonality

We found that the vertical nitrate flux in winter predicted the pre-bloom nitrate pool remarkably well (Fig. 4A). Consequently, deep winter mixing, where it occurs, dominates the annual nitrogen budget (Fig. 3), expanding on direct measurements of a full annual cycle over the Barents Sea shelf break (Randelhoff et al., 2015). Hence, potential advective processes do not play as large a role at Pan-Arctic scales, at least at the locations and times investigated here. Our results explicitly and quantitatively confirm the qualitative perception that vertical nitrate fluxes determine the seasonality of the upper ocean nitrate inventory, as has been surmised multiple times in the literature (see e.g. Carmack and Wassmann, 2006; Tremblay et al., 2015) based on general considerations of stratification and bathymetry.

Stratification and bathymetry also governed pre-bloom surface nitrate concentrations (Fig. 4B) and hence, by extension from the aforementioned, vertical nitrate fluxes. Specifically, locations with the same strength of upper-ocean stratification had on average consistently highest pre-bloom nitrate over the shelf slope (200 m < depth < 1500 m), lower on the shelves (< 200 m), and lowest over the basins (>1500 m). These findings correspond to general expectations as rough or shallow topography provides more opportunities for currents to interact with the bathymetry. Indeed, mixing in the Arctic has been found to be especially elevated over the shelf slope (Rippeth et al., 2015), and for instance tidal velocities are generally higher over the shelves than over the deep basins (Kowalik and Proshutinsky, 2013).

4.2 Primary production constrained by nitrate fluxes

The close match between nitrate fluxes and nitrate inventory demonstrates the eminent role of stratification and turbulence in Arctic Ocean nutrient dynamics. The real value of measuring nitrate fluxes, however, lies in constraining primary production.

The most commonly employed notion of “primary production” is “net primary production” (NPP), comprised of both new and regenerated production (see Appendix, Fig. 9). Where nitrogen is scarce in summer, regenerated production is a significant if not dominant fraction of NPP. Hence NPP is significantly larger than the amount of inorganic nitrogen that is converted into organic matter, which is the quantity than can be reasonably expected to be constrained by nitrate fluxes. Indeed, for one ocean colour remote sensing algorithm (Arrigo and van Dijken, 2015), net primary production was at least an order of magnitude larger than the corresponding wintertime nitrate fluxes (see Supplementary Material).

4.2.1 Annual basin-scale productivity

Two other measures of primary production are more directly related to the assimilation of inorganic into organic nitrogen: First, new production (Dugdale and Goering, 1967), which relies only on nitrate brought up from below the photic zone. It is customarily measured by incubating phytoplankton in seawater spiked with some nitrate, using a radioisotope to track its incorporation into organic matter (Collos, 1987). Second, export production (Eppley and Peterson, 1979), which in its most basic form is measured as the downward particle export over a given time interval using sediment traps (Zeitzschel et al., 1978). This number is stipulated to be similar to the upward nitrate flux based on conservation of mass alone.

Over seasonal time scales, both the upward nitrate flux in winter, the particle export at 200 m depth, and new production (nitrate uptake) matched up reasonably well for Baffin Bay, the Barents Sea, the Southern Beaufort Sea, and the Central basin (Fig. 5), both in regional patterns and order of magnitude. Other regions lack estimates of the winter nitrate flux. Indeed, annual budgets have to be closed if nitrate inventories are not to change in the long term. The differences between export production, new production, and the vertical nitrate flux hence likely reflect the extreme disparity of spatial and temporal scales of the different measurements. However, no study has systematically investigated all three quantities on annual to interannual time scales and at the same location.

4.2.2 Short-term new production

A somewhat different matter is the hypothesis that during the summer, upward mixing of nitrate limits the amount of new production in the short term. Here, the published literature gives a less clear picture (Fig. 6A). Randelhoff et al. (2016) measured vertical nitrate flux and new production for both spring and summer in the marginal ice zone around northern Fram Strait. In spring, uptake of nitrate was considerably larger than its vertical supply as nitrate was not yet depleted and hence did not limit photosynthesis. In summer, on the other hand, when the surface water was nitrate-depleted, new production was an order of magnitude *smaller* than nitrate supply, contrary to the hypothesis.

A likely contribution to this discrepancy was the seasonal buildup of dissolved organic nitrogen (Fig. 6B) observed during the same field campaigns by Paulsen et al. (2018), although the explanation is probably composite. Taken together, our findings hence stressed the importance of the recycling of nitrogen in the microbial loop when considering nutrient fluxes over short subseasonal time scales. The nitrate uptake rate measurements by Randelhoff et al. (2016) only considered assimilation into the particulate pool due to methodological constraints. Nishino et al. (2018) found good agreement between upward nitrate flux, nitrate uptake, and export of particulate organic matter, based on a case study in the Chukchi sea. This may represent geographic differences in the dynamics of the system, or even in the methodology. Nishino et al. (2018) used different methods from those of Randelhoff et al. (2016), even though they neglected assimilation into the dissolved nitrogen pool as well (Shiozaki et al., 2009).

Our measurements in Young Sound, North-East Greenland (see Appendix), gave a diametrically opposed view: Here, vertically integrated new production was significantly above the vertical turbulent supply of new nitrate in this extremely quiescent fjord. Indeed, it is likely strong stratification and hence weak vertical mixing in Young Sound that limits overall productivity (Holding et al., 2019). Tidal mixing over the two shallow sills in concert with isopycnal mixing may aid with the overall upward nitrate supply (see e.g. Fer and Drinkwater, 2014), but terrestrial runoff may also contribute significantly to the nutrient cycling (Rysgaard et al., 2003) as nitrate concentrations in run-off water are higher than those measured in the sea surface (Paulsen et al., 2017). This scenario is likely specific to this fjord and cannot be generalized around Greenland as nitrate concentrations in Greenland Ice Sheet run-off often act to dilute surface nitrate concentrations (Hopwood et al., 2019).

In the same vein, but outside the Arctic Ocean, Law et al. (2001) and Rees et al. (2001) found that vertical mixing supplied only 33 % of the nitrate demand at a North Atlantic site, in agreement with a study by Horne et al. (1996) in the Gulf of Maine. Even in the Mauritanian upwelling region, nitrate fluxes in excess of 100 mmol N m^{-2} d^{-1} accounted for only 10-25% of observed net community production (Schafstall et al., 2010). Yet more extremely, Shiozaki et al. (2011) found that one location on the continental shelf of the East China Sea “exhibited a considerable discrepancy between the nitrate assimilation rate (1500 mmol N m^{-2} d^{-1}) and vertical nitrate flux (98 mmol N m^{-2} d^{-1})”, and they went so far as concluding that “the assumption of a direct relationship between new production, export production, and measured nitrate assimilation is misplaced, particularly regarding the continental shelf of the East China Sea”.

The scarcity of dedicated measurements that evaluate both nitrate fluxes, new production, and organic nitrogen pools at relevant space-time scales is the major impediment to evaluating the direct impact of nitrate fluxes on primary productivity in the Arctic on time scales of days. However, given the correspondence we established between annual new production and vertical nitrate supply over Pan-Arctic scales, any mismatch between the two is likely reflected in asynchronous seasonal patterns of the different nitrogen pools (Figs. 6, 9B). Phytoplankton growth responses may also lag nutrient supply pulses, perhaps necessitating time series approaches when studying scales as short as weeks (Omand et al., 2012).

5 Future scenarios

5.1 Nitrogen limitation of primary production

Nitrogen scarcity plays a large role in constraining Arctic marine primary production (Moore et al., 2013; Tremblay et al., 2015). Nutrient limitation of phytoplankton growth is usually quantified in terms of a *half-saturation constant* (of a Michaelis-Menten kinetics), above which nutrient uptake rates benefit less and less from increasing ambient nutrient concentrations. Reported values of such half-saturation constants vary widely according to species and physiological state, but reasonable values usually cluster around an order of magnitude of 1 µM (e.g. Wassmann et al., 2006). Hence we infer that nitrate limitation holds across large swaths of the Arctic, but not including some of the central basin, where summer surface concentrations are in excess of e.g. 5 µM in the Makarov and Nansen basins (Fig. 7). These high nitrate concentrations in the Central Arctic are usually taken to indicate regionally important light limitation by perennial sea ice cover (Codispoti et al., 2013).

Regarding nitrate concentrations as indicators of potential growth however, a cautionary remark is in order. Since the nitrate supply, like phytoplankton growth, is a rate and not a stock, its present-day inventory alone does not yield sufficient information to infer possible limitations in future scenarios. Hence the summer surplus nitrate that is observed in the central AO may only be available transiently while the ice cover shrinks, but not in a steady-state situation without summer sea ice. Similarly, a deeper euphotic zone (e.g. due to a more transparent ice cover) could enhance growth in subsurface waters, richer in nutrients, but the resupply rate of nitrogen ultimately decides about potential lasting increases in new production.

Randelhoff and Guthrie (2016) provided estimates of end-of-century new production, given presently observed turbulence and potential future increases in stratification observed in a numerical circulation model (Nummelin et al., 2015). They concluded that there could be an approximately 50% increase in new production in the Amundsen Basin if the system were to turn to nitrate limitation under unchanged stratification; they cautioned, however, that most of that increase may fall victim to future increases in stratification which in turn decreases fluxes. In general, stratified areas with higher influence of riverine or pacific freshwater may get even more stratified and hence more nitrogen-limited, but that concerns mainly the interannual background stratification. Little is known about the future of seasonal and especially summertime stratification (Randelhoff et al., 2017).

Contrarily, Polyakov et al. (2017) posited that an ongoing Atlantification will lead to deeper winter convection in the Eurasian Basin. In fact, Atlantic water, being less stratified, is associated with high nitrate fluxes (Randelhoff et al., 2015). A spreading of Atlantic waters into the central AO could hence add to the upper-ocean nitrate pool, but no estimates of the magnitude of that effect have been published to our knowledge. As Atlantic Water is also the principal source of heat in the Arctic Ocean, it has been implicated in recent sea ice loss (Ivanov et al., 2016; Polyakov et al., 2017), and hence could regionally relieve nutrient and light limitation at the same time (Randelhoff et al., 2018). The recent decreases of sea ice extent in Northern Fram Strait and north of Svalbard (Onarheim et al., 2018) indicate that such a process is already well underway. The analogue may be happening in the Chukchi sea, where the Alaskan Coastal Current brings in both large amounts of heat (Woodgate et al., 2012) and nutrients (Torres-Valdés et al., 2013), but the published literature seems to be less clear on the presence and effects of such a tentative advective borealization of the Chukchi sea.

5.2 Ice cover and wind-driven turbulence

A decreasing sea ice cover has been hypothesized to enhance the input of wind energy into the ocean (Dosser and Rainville, 2016), but increasing stratification resulting from higher ice melt rates will likely counteract the resulting increased mixing (Randelhoff et al., 2017).

More concretely, based on a two-year mooring timeseries of velocity observations on the shallow Chukchi shelf, Rainville and Woodgate (2009) showed that during the period of heavy winter ice cover, water velocities, and consequently turbulent mixing, were strongly reduced. While less ice cover did in fact enhance input of wind energy in the perennially stratified Beaufort Sea basin in observations by Lincoln et al. (2016), little of that mixing lead to increases in fluxes from the intermediary warm, nutrient-rich layers due to the strong stratification. The strong stratification was also the hypothetical explanation by Guthrie et al. (2013) for the lack of change in current profiler-inferred mixing estimates compared to historical records in the central Arctic Ocean basin. Similarly, Chanona et al. (2018), analyzing CTD profiles collected in the Canadian Arctic using an internal-wave based finescale parameterisation, found a weak seasonal cycle in dissipation of turbulent kinetic energy, but no interannual trend from 2002 through 2016.

In summer, when ice is broken up and in more or less free drift, wind energy input into the upper ocean may even be higher in ice-covered than open water areas (Martin et al., 2016). Hence retreating summer sea ice may not immediately lead to increased rates of turbulent energy dissipation. A retreat of winter sea ice would, however, decrease the extent of low-salinity water layers in the upper tens of meters during the following melt period (Randelhoff et al., 2017). This is demonstrated by the fact that Randelhoff et al. (2016) measured nutrient fluxes approximately twice as high in the open-water stations in the Marginal Ice Zone compared to those covered by melting sea ice. Hence, changing upper ocean stratification may ultimately lead to larger changes in vertical nutrient transport than the potentially minor difference between input of mixing energy through open water and through summer sea ice. A major uncertainty for future prognoses is the scarcity of large-scale surveys of the ice-ocean boundary layer which is hard to access from large vessels, a notable exception being the airborne SIZRS campaigns described by Dewey et al. (2017).

While these increased open water fluxes were close to negligible in terms of total annual nitrate supply, they may slightly relax nutrient limitation during the summer and hence alter plankton community composition (Li et al., 2009). In addition, under sea ice, irradiance is strongly reduced but its variability enhanced, likely exacerbating such changes in community composition. Lastly, if the overall loss of sea ice eventually leads to drastic changes in background stratification, nutrient fluxes would change as well.

5.3 Arctic nitrate fluxes in a global context

Based on a literature review (Table 2), Arctic vertical nitrate fluxes tend to be approximately one order of magnitude lower than in the rest of the world ocean (Fig. 8). Even though study sites in the global ocean may be biased by measurements seeking to explain high biological productivity (most often as the result of strong mixing), this simple comparison demonstrates the considerable gap between potential for new and hence harvestable production in most of the Arctic Ocean and the world's fishery grounds.

6 Conclusions

6.1 Summary

1. Determining nitrate fluxes is a laborious task. With measurements accumulating through the last 10 years, we are now approaching a Pan-Arctic baseline. In individual regions however, perhaps with the exception of the Barents Sea, seasonal coverage remains patchy at best.
2. Arctic nitrate fluxes are, on average, one to two orders of magnitude smaller than those observed elsewhere in the world ocean.
3. The spatial patterns of the upper ocean nitrate inventory are well explained by vertical nitrate fluxes, and the seasonality in this inventory is reflected in the seasonality of the nitrate fluxes.
4. Nitrate fluxes are a powerful tool to constrain export fluxes and new production, both of which are hard to measure autonomously. There is an important distinction between "(net) primary production" and "new production", highlighted by the fact that the former is considerably larger than annual nitrate supply.
5. On weekly or shorter timescales, the relation between nitrate supply and new production is unclear, mostly due to lack of appropriate time series data. A certain asynchronicity between the different nitrogen pools may confound budget calculations.

6.2 Avenues for further research

Besides further aggregate scale (seasonal or basin-scale) measurements of the turbulent vertical nitrate flux, two avenues emerge from our conclusions.

1. Advances in turbulence-ecosystem coupling will require dedicated or autonomous sampling and time series. Physically-oriented turbulence sampling often does not sufficiently resolve the biologically relevant surface layer.
2. Prediction of upper ocean mixing and ice-ocean interaction depends on sea ice melt and freeze rates, in units of meters of freshwater equivalent per unit area. Yet, to our knowledge,

this quantity is not routinely investigated as output of coupled ice-ocean circulation models and hence no such data product exists that could aid in the extrapolation of Pan-Arctic patterns of the seasonal vertical nitrate flux.

6.3 Nitrate fluxes in diagnosis and prognosis of primary production

While currently publicly available datasets are more comprehensive for new and export production (Stein and MacDonald, 2004) than for nitrate fluxes, they possess some drawbacks concerning evaluating large-scale patterns. Incubations to determine new production are usually point measurements, and hence averaging them is not trivial. Sediment traps, while measuring export fluxes at a single location, integrate the time dimension, and are hence more representative, but also require a large logistic effort. Chemical tracer approaches (e.g. Moran et al., 2003) make the data acquisition phase easier, but still require water samples and are hence not easily amenable to autonomous exploration. In sum, current Arctic Ocean exploration does not scale well. NO_3^- fluxes, on the other hand, can be estimated purely based on physical sensor data and hence with larger scope both in time and space.

Such turbulence measurements do not necessarily have to be conducted using microstructure profilers - mixing can also be estimated from current shear or density strain fine-structure with more standard instruments, which may work especially well in discerning relative magnitudes but can also be calibrated using regional microstructure estimates (Chanona et al., 2018; Gargett and Garner, 2008; Guthrie et al., 2013; Polzin et al., 2014). Parameterizations of this kind, relying on models of internal wave breaking, are most useful away from boundaries, hence for scenarios of perennial stratification where year-round background fluxes dominate (Randelhoff and Guthrie, 2016), and less so to characterize near-surface mixing. Other promising avenues are approaches based on turbulence structure functions (Wiles et al., 2006), high-frequency ADCP measurements, or microstructure sensors deployed on moorings and gliders (Scheifele et al., 2018).

Turbulence also obeys tight physical constraints imposed by wind, tidal and other energy available for mixing, and by the freshwater (density) fluxes that cause background stratification. Hence nitrate fluxes are more easily constrained than plankton photophysiology that is notoriously variable across species and environmental conditions (e.g. Bouman et al., 2018).

6.4 Perspectives

This study has focused on vertical diffusive transport. Upwelling, horizontal advection, mesoscale eddy shedding, benthic processes, and the biogeochemistry of the catchment basins are other factors likely affecting Arctic Ocean primary production at least regionally.

Mesoscale turbulence can contribute to cross-shelf transport and nutrient supply in the Chukchi sea (Watanabe et al., 2014). Some studies suggest that eddies may also contribute to cross-shelf transport along the West Spitsbergen Current (Hattermann et al., 2016). Crews et al. (2018) found eddies may contribute to ventilation of halocline waters in the European Arctic, meaning they would be apparent in the upward vertical fluxes measured out of the halocline waters instead of contributing directly to mixed-layer nitrate pools. Johnson et al. (2010), working in the Subtropical North Pacific, stressed the importance of event-driven upward nitrate transport not easily captured by vertical diffusivities, and even the possibility of immediate utilisation of nitrate in an otherwise diabatic isopycnal excursion, for example associated with a passing eddy. Attention is required summing these contributions, however, as there is a certain danger of double counting nitrate fluxes in eddies (Martin and Pondaven, 2003; Martin and Richards, 2001).

Coastal areas and the shallow shelves, affected by permafrost mobilization and sea ice decreases, may see large changes compounded by changes in benthic communities (Renaud et al., 2015) and river biogeochemistry (Frey and McClelland, 2009).

Advection with ocean currents manifests itself largely as transport with the Pacific and Atlantic currents that e.g. Torres-Valdés et al. (2013) have discussed. For the most part, these currents are subducted under local (Arctic) water masses and can hence be accounted for as part of the vertical fluxes downstream. Randelhoff et al. (2016) have argued that as these currents come from further south where primary production starts earlier and terminates later, the surface waters they carry are as nutrient-depleted as the Arctic surface waters. This argument has, however, never been tested quantitatively. Similarly, upwelling along coasts, shelf breaks and in eddies may also contribute regionally to ocean productivity (Carmack and Chapman, 2003; Kämpf and Chapman, 2016; but see Randelhoff and Sundfjord, 2018). Arguments have largely remained qualitative with respect to the exact pathways and nutrient budgets (but see Spall et al., 2014 for a careful modelling exercise).

The fact that Pan-Arctic patterns of primary production can seemingly be explained without the need to invoke any of these mechanisms also showcases the stark contrasts between the different Arctic regimes that likely shadow intra-regional nuances. Lastly, turbulent mixing is much more than only the vertical nitrate flux. It affects predator-prey interactions, nutrient uptake rates at the cell level, light exposure of individual cells, etc. In fact, mixing and variability is a resource in itself that can be exploited by different plankton life strategies. These concepts may turn out to be important in particular when interpreting regional specifics such as biological hotspots. As methods advance and measurements accumulate, we expect that more efforts can be dedicated to studying regional phenomena in a Pan-Arctic unified manner.

7 Conflict of Interest

The authors declare that the research was conducted in the absence of any commercial or financial relationships that could be construed as a potential conflict of interest.

8 Author Contributions

AR designed the study, made all visualizations, and wrote the first draft of the manuscript. AR, JMH, and MS conducted field sampling and data analysis of the Young Sound data. MBA and MJ conducted sampling and data analysis of the Laptev Sea data. JET contributed Canadian Archipelago nutrient data. All authors commented on the manuscript.

9 Funding

Data acquisition of BGC-Argo Floats in Baffin Bay was led by M. Babin and funded through the NAOS project. Work in Young Sound was supported by the DANCEA project “De-icing Arctic coasts” and the Greenland Ecosystem Monitoring Programme. AR was supported by the Sentinel North program of Université Laval, partly funded by the Canada First Research Excellence Fund, and CARBON BRIDGE: Bridging marine productivity regimes: How Atlantic advective inflow affects productivity, carbon cycling, and export in a melting Arctic Ocean, a Polar

Programme (project 226415) funded by the Norwegian Research Council. JMH was supported by the European Commission H2020 programme under the Marie Skłodowska-Curie Actions (GrIS-Melt: grant no. 752325). MBA was supported by the National Science Foundation (PLR-1203146 AM003) and the National Oceanic and Atmospheric Administration (NA15OAR4310156).

10 Acknowledgments

The present paper started taking shape around the 4th "Symposium on Pan-Arctic Integration", held in Motovun, Croatia, 2017, and we thank all participants for inspiring discussions.

We thank Andrey Novikhin (AARI) for preparing the nutrient measurements from the Laptev Sea shelf, Xiaogang Xing for quality-controlling and calibrating the Baffin Bay BGC Argo data, and Jørgen Bendtsen and Torben Vang for providing Young Sound bathymetry data. We are further grateful to Shigeto Nishino for clarifying discussions about his work in the Chukchi Sea.

Data exploration and visualization relied heavily on the Holoviews library (Stevens et al., 2015).

11 Supplementary Material

The supplemental material, accessible at https://github.com/poplarShift/arctic-nitrate-fluxes, contains:

- The python code necessary to reproduce all analyses and figures, licensed under GNU GPL3.
- The data, as plotted in all figures, in machine-readable formats.
- An interactive version of this article where figures can be zoomed, panned, and selectively highlighted (as appropriate) leveraging the Bokeh library (Bokeh Development Team, 2018).

12 Data Availability Statement

All data that were published for the first time in this study are included with the above repository. The rest are included to the extent possible.

13 Appendix

13.1 The marine nitrogen cycle

Discussions of ocean surface nitrogen budgets center around the marine nitrogen cycle. Fig. 9 shows a simplified version adapted to Arctic conditions. The main component is the cycling between inorganic nitrate and particulate organic nitrogen (PON). Upward transport of NO_3^- compensates nitrate uptake by algae into PON (Dugdale and Goering, 1967) and subsequent sinking of this organic matter. The loop is closed by remineralization into nitrate at depth. When nitrogen is scarce in the surface layer, there is also intense recycling of nitrogen that has already been assimilated into organic matter, which is called regenerated production.

Additional complexity arises from a number of sources, sinks, and recycling processes not accounted for in this simplistic view. One of the conclusions of the present study is that we do not need to invoke those processes to understand Arctic surface layer budgets on a Pan-Arctic scale. However, processes like advection, upwelling, mesoscale mixing, nitrification, denitrification, or nitrogen fixation, may be important depending on the regional scope. Riverine inputs of nitrate are thought to be sufficiently small to be neglected at larger-than-regional scales (see e.g. Tank et al., 2012). Some of the produced PON is also harvested e.g. by higher trophic levels or fisheries (e.g. Valiela, 2015), although the latter process is likely only regionally important, e.g. in the Barents Sea.

13.2 The vertical layering of Arctic Ocean nitrate

Fluxes are easiest to measure across strong gradients. A given vertical profile of nitrate concentrations in the Arctic Ocean can schematically be vertically divided by two nitraclines (Fig. 9A): First, a seasonal one, which marks the transition from surface waters, modulated by seasonal freshwater from ice melt or terrestrial runoff and algal growth, to the remnant winter mixed layer. Second, and mostly present in the deep basins of the Arctic Ocean, one that we dub “perennial” as it is not eroded and re-established on an annual basis.

The seasonal nitracline may be completely mixed during winter (Fig. 9B), rendering fluxes hard to estimate using the “diffusivity times gradient” formula. Across the perennial nitracline, fluxes can be estimated year-round stipulating the seasonal variations in nitracline dissipation are minor, a method exploited by Randelhoff and Guthrie (2016) to estimate Pan-Arctic patterns of upward nitrate supply in the deep basin. In practice, the two nitraclines are often not clearly delineated. The distinctive characteristics of the two nitraclines are most easily seen in the Eurasian Basin, where deep winter mixed layers are clearly separated from underlying Atlantic Waters. In the Canadian Basin, strong stratification prevents winter mixing from penetrating deep into the nitracline (Peralta-Ferriz and Woodgate, 2015), leading to relatively small seasonal excursions in surface nutrient concentrations and a less distinct winter remnant mixed layer (Fig. 9C).

13.3 Measuring vertical nitrate fluxes

Barring regionally important processes such as upwelling and eddy pumping (Carmack and Chapman, 2003; Kämpf and Chapman, 2016; Randelhoff and Sundfjord, 2018), the most prevalent form of the upward transport of nitrate in the ocean is turbulent diffusion (Lewis et al., 1986). Such diffusion mixes the spent surface waters with deeper, more nutrient-rich waters, thereby replenishing their nitrate reservoir. A vertical turbulent nitrate flux is, by definition, the product of a so-called “diapycnal eddy diffusivity” with the vertical gradient of nitrate. (This is completely analogous to any other tracer such as temperature or salinity. The interested reader is referred to the vast literature on turbulent flows.)

To estimate both those quantities, one has to measure the turbulence and a vertical profile of nitrate concentrations at the same time and location. Determining nitrate is comparatively uncomplicated because only the non-turbulent background is needed; one can use either bottle samples or, preferably, optical nitrate sensors to achieve a better vertical resolution (Alkire et al., 2010; Randelhoff et al., 2016). Both of these options are easily integrated into standard sampling with a CTD rosette. While care should be taken to calibrate the absolute concentrations of optical sensors against water samples, such biases are usually depth-independent and hence do not matter for the calculation of the gradients (see Appendix of Randelhoff et al., 2016). Measuring turbulence is more challenging because it requires either measurements with sophisticated instruments, requiring dedicated ship time and personnel, or parameterizations that add layers of uncertainty (e.g. Garrett and Munk, 1975; Guthrie et al., 2013).

13.3.1 Measuring turbulence

The most direct way of determining a nitrate flux is measuring the so-called "dissipation of turbulent kinetic energy" (ϵ) traditionally using free-falling microstructure profilers (Lueck et al., 2002). ϵ can also be estimated from larger-scale current shear or strain visible in CTD profiles (Guthrie et al., 2013), even though that adds another layer of parameterizations. Once ϵ is determined, its accuracy usually cited as being within a factor of two (Moum et al., 1995), the vertical turbulent diffusivity can be calculated, following Osborn (1980), as

$$K_\rho = \Gamma \frac{\epsilon}{N^2} \qquad (1)$$

where N^2 is the Brunt-Väisälä buoyancy frequency and $\Gamma \approx 0.2$ is the mixing coefficient that reflects how much of ϵ is available for adiabatic mixing. Eq. 1 has a number of known issues, a major one being that Γ is not constant. A variety of different parameterizations have been proposed (e.g. Shih et al., 2005; Bouffard and Boegman, 2013), with no clear alternative emerging. Eq. 1 is hence the de facto standard (Gregg et al., 2018), and in fact all turbulence-based estimates of the vertical nitrate flux compiled for this paper are based on it, albeit e.g. Sundfjord et al. (2007) determined the value of Γ that best fit their observations using a detailed analysis of microstructure data.

13.3.2 Using the inorganic nitrate drawdown as an indicator of nitrate flux

Another method to determine vertical nitrate fluxes, less direct, uses a set of nitrate profiles through fall and winter (Randelhoff et al., 2015). It has been employed to calculate two of the fluxes presented in this study. Vertically integrating the successive differences between them, one essentially reverses the calculation of net community production by the nitrate drawdown between winter and summer (Codispoti et al., 2013). Randelhoff et al. (2015) provided a brief overview over potentially interfering processes such as nitrogen fixation (Blais et al., 2012) and concluded they were likely not significantly disturbing the annual budgets, but it has to be acknowledged that data is sparse. While this method may be robust in the pelagic, one can doubt its effectiveness in waters where nitrogen cycling is heavily affected by other processes, such as benthic processes in shallow waters, or coastal effects.

13.4 New estimates of nitrate fluxes and new production in Young Sound, NE Greenland

13.4.1 Methods

Sampling in the Young Sound/Tyrolerfjord system was conducted during three weeks in August 2015 from the Daneborg research station as part of the Danish MarineBasis program in Zackenberg (Fig. 10A).

Water column nutrient samples were taken at 5 stations using a manually operated Niskin bottle from depths of 1, 5, 10, 20, 30, 40, 50, and 100 m. They were filtered with Whatman GF/F filters before being stored in previously acid-washed 30 mL high-density polyethylene (HDPE) plastic bottles and frozen until analysis (-18 °C). Nitrite (NO2) and nitrate (NO_3^-) concentrations in each sample were measured on a Smartchem200 (AMS Alliance) autoanalyzer.

An MSS-90L (Sea and Sun Technology, Germany) free-falling microstructure profiler was deployed at a total of 37 stations, many of them repeat stations, to measure vertical profiles of the dissipation of turbulent kinetic energy. At the same stations, we deployed a SUNA (Satlantic) nitrate spectrophotometer to collect co-located vertical profiles of nitrate concentration. SUNA profiles were post-processed following (Randelhoff et al., 2016) and calibrated using a constant bias determined from comparison with the nutrient water samples.

New and regenerated production were investigated at a subset of five stations. They were measured in two parallel incubations, labelled with ca. 10% ambient concentration of $^{15}NO_3^-$ and $^{15}NH_4^+$ respectively. Water samples were incubated in triplicate 500 ml polycarbonate bottles in situ. Additionally ca. 10% ambient concentration of ^{13}C-bicarbonate was added to both sets of incubations to follow the incorporation of inorganic carbon into biomass. Samples were taken for NO_2^-+NO_3^- , $^{15}NO_3^-$ and $^{15}NH_4^+$ before and after addition of tracers by filtering through a syringe filter (Whatman GF/C) into 10 ml polystyrene vials which were frozen (-18 °C) until analysis. After the incubation the particulate matter from each incubation vessel was filtered onto pre-combusted GF/F filters and later the ^{15}N and ^{13}C content of the particles on the filters was determined by mass spectrometry. Before filtration a third set of samples for NO_2^-+NO_3^-, $^{15}NO_3^-$ and $^{15}NH_4^+$ were taken. NO_2^-+NO_3^- was determined photometrically following Schnetger and Lehners (2014). $^{15}NH_4^+$ was determined based on Risgaard-Petersen et al. (1995). $^{15}NO_3^-$ was determined as in Kalvelage et al. (2011). New and regenerated production were calculated as the ratio of nitrate or ammonium to total N-uptake in each incubation respectively multiplied by the total C-uptake in each incubation.

In total, we collected 43 profiles of co-located SBE25+SUNA profiles, 103 MSS casts, 40 nutrient bottle samples and 20x3 triplicates of new and regenerated production incubations.

13.4.2 Results

A freshwater layer was present throughout the fjord, but most prominent in the innermost parts (Fig. 10B-D). Nitrate was depleted throughout the upper 40 m, below which concentrations steeply rose to about 4 µM. The fjord was remarkably quiescient in terms of turbulent dissipation rates, but mixing was significantly elevated over the sills. Vertical nitrate fluxes, computed for each station of co-located MSS and SUNA measurements, ranged from 0.012 to 13.26 mmol N m^{-2} d^{-1}, with some of the values in the fjord interior being the lowest observed across this entire study. Median upward fluxes were 0.036 and 0.33 mmol N m^{-2} d^{-1} in the fjord interior and over the sills, respectively. Incubations, although only available at two depths (5 and 20 m), indicated new production rates on the order of 0.1 to 1 mmol N m^{-2} d^{-1} (Fig. 10E).

13.5 Nitrate flux estimate in the Laptev Sea

13.5.1 Data description

Microstructure and nutrient measurements from the Laptev Sea were collected under the framework of the German-Russian "Laptev Sea System"-partnership in 2008, 2011, 2014, and 2018 (Fig. 11B). The 2008-winter profile was averaged from measurements collected during the helicopter-supported "Transdrift 13" winter expedition (6 April to 10 May 2008) to the southeastern Laptev shelf. The summer nitrate profile was averaged from profiles collected during the "Transdrift 19" expedition on board the RV Jakov Smirnitsky in September 2011 (Bauch et al., 2018).

In 2014 microstructure turbulence profiles were collected on 19 September 2014 during the Transdrift 22-expedition aboard the RV Viktor Buinitsky (see Janout et al., to be submitted to this issue). The dissipation rates of turbulent kinetic energy (ϵ) were derived from shear variance measured with a freely falling MSS-90L microstructure profiler manufactured by Sea and Sun Technology (SST, Germany). Vertical profiles of epsilon were calculated from the isotropic formula and spectral analysis of 1-s segments and subsequently averaged into 1-m bins. Turbulent vertical fluxes are based on a diapycnal eddy diffusivity with a constant mixing efficiency taken to be 0.2 (Osborn, 1980). For statistical robustness, the 2014 MSS profile shown in this paper was averaged from a series of five casts.

In 2018 a joint German-US-Russian expedition to the Eurasian Arctic was carried out aboard the RV Akademik Tryoshnikov from 18 August to 30 September 2018. The expedition combined the German-Russian CATS (Changing Arctic Transpolar System) and the US-Russian NABOS (Nansen Amundsen Basin Observing System) programs. The dissipation profile was again generated with a MSS-90L, while the nitrate profile was recorded with a Deep SUNA V2 nitrate profiler (Seabird Scientific) attached to the shipboard CTD/rosette. These data files were then processed using a program (ISUSDataProcessor) developed by Ken Johnson (MBARI) that corrects the spectral data for temperature effects on the bromide absorption and applies a linear baseline correction to account for absorption by colored dissolved organic matter (Sakamoto et al., 2009). SUNA nitrate concentrations were then compared with nitrate concentrations measured from discrete seawater samples collected at various depths above 20 and below 300 m depth where concentrations were sufficiently constant with depth. The full description of the methods is distributed with the data (Alkire, 2019).

13.5.2 Nitrate fluxes

Two representative profiles were selected to compute nitrate fluxes (Fig. 11A): Cast 59 and a co-located MSS profile, both sampled in 2018, and the 2014 MSS profiles and cast 62, also co-located but from separate years. For both profiles, we visually determined the nitracline, averaged ε over that interval, and computed the average nitrate and density gradients by a linear regression. The resulting nitrate fluxes were 0.014 and 0.017 mmol N m^{-2} d^{-1}, and hence we entered the average value of 0.015 mmol N m^{-2} d^{-1} for the Laptev Sea into the nitrate fluxes compilation.

13.6 Nitrate flux estimate in Baffin Bay

Three biogeochemical Argo floats, part of the NAOS project, overwintered in Baffin Bay from July 2017 to July 2018, described in detail by Randelhoff et al. (2019, in prep.).

Nitrate concentration was observed by the Satlantic Submersible Ultraviolet Nitrate Analyzer (SUNA). Each sensor's offset, taken to be constant and depth-independent (Randelhoff et al., 2016), was corrected based on nitrate concentration profiles sampled during deployment of the floats. Mixed layer depth was defined as the shallowest depth where density rose more than 0.1 kg m^{-3} above the surface density.

Integrating the nitrate deficit $\Delta[NO_3{}^-] \equiv [NO_3{}^-](60m) - [NO_3{}^-](z)$ over the upper 60 meters for each station shows that over the course of four months (from November to March), a deficit of 200 mmol N m^{-2} was replenished, approximately equivalent to an upward nitrate flux of 1.66 mmol N m^{-2} d^{-1} (Fig. 12). The usual caveats about neglecting mixed-layer regeneration of nutrients apply, and hence this calculation makes the same kind of assumptions as have been detailed by Randelhoff et al. (2015).

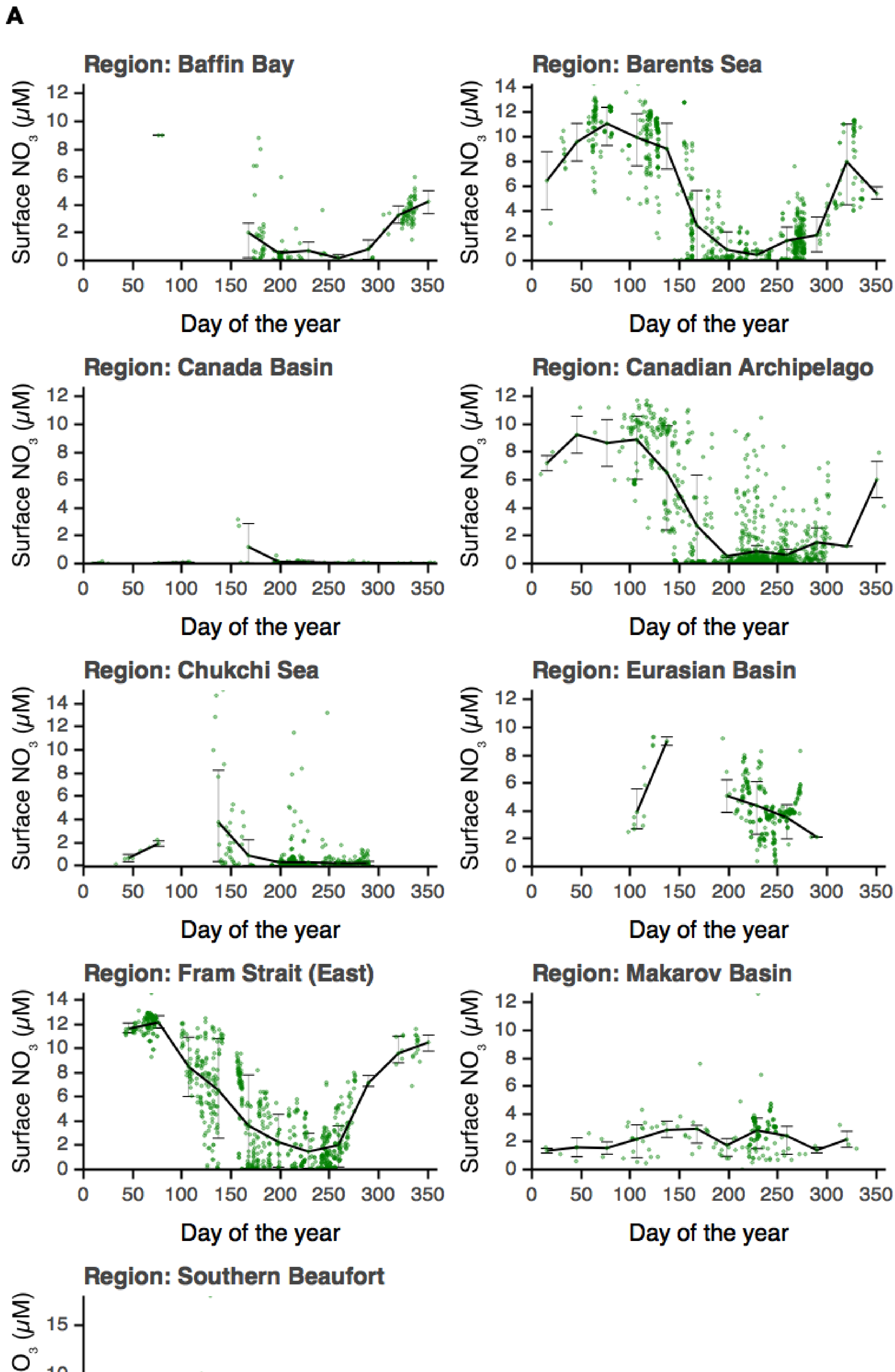
A
Region: Baffin Bay
Region: Barents Sea
Region: Canada Basin
Region: Canadian Archipelago
Region: Chukchi Sea
Region: Eurasian Basin
Region: Fram Strait (East)
Region: Makarov Basin
Region: Southern Beaufort
Surface NO_3 (μM)
Day of the year
0 50 100 150 200 250 300 350

Figure 1: (A) Seasonal cycles of surface nitrate concentrations in different regions of the Arctic. (B) The delineation of these regions largely follows Codispoti et al. (2013) and Peralta-Ferriz and Woodgate (2015).

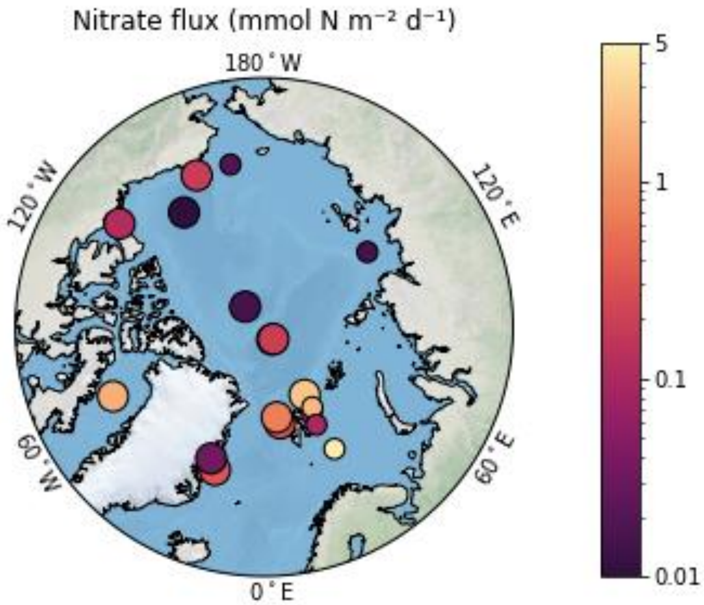

Figure 2: All nitrate flux compilation across the AO compiled for this study, irrespective of season and vertical levels. The smaller dots indicate single stations, whereas the big dots represent averages over larger time or space scales.

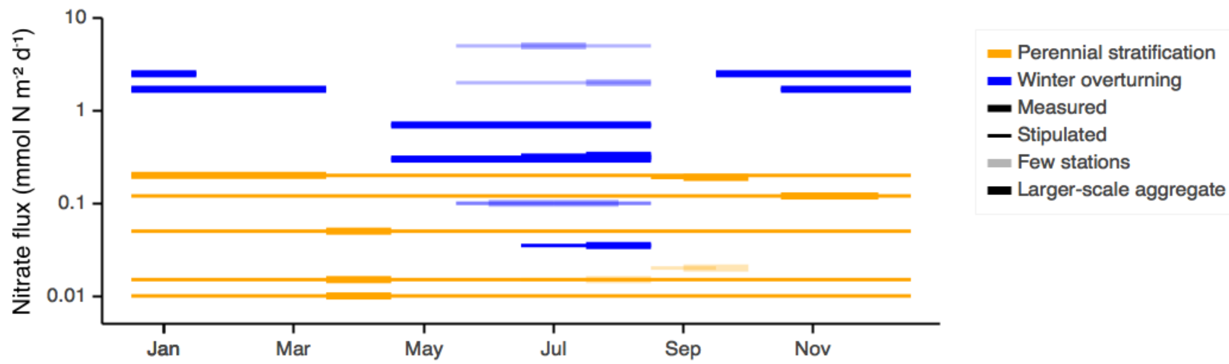

Figure 3: Nitrate fluxes as a function of the month. Blue lines mark the regions where the water column overturns in winter and orange those where it does not. Thick lines represent measurements, whereas thin lines denote values (stipulated by the authors) that extrapolate the measured fluxes based on general considerations about stratification and the seasonality of primary production. Pale lines reflect single stations, potentially not very representative of the regional or seasonal scale.

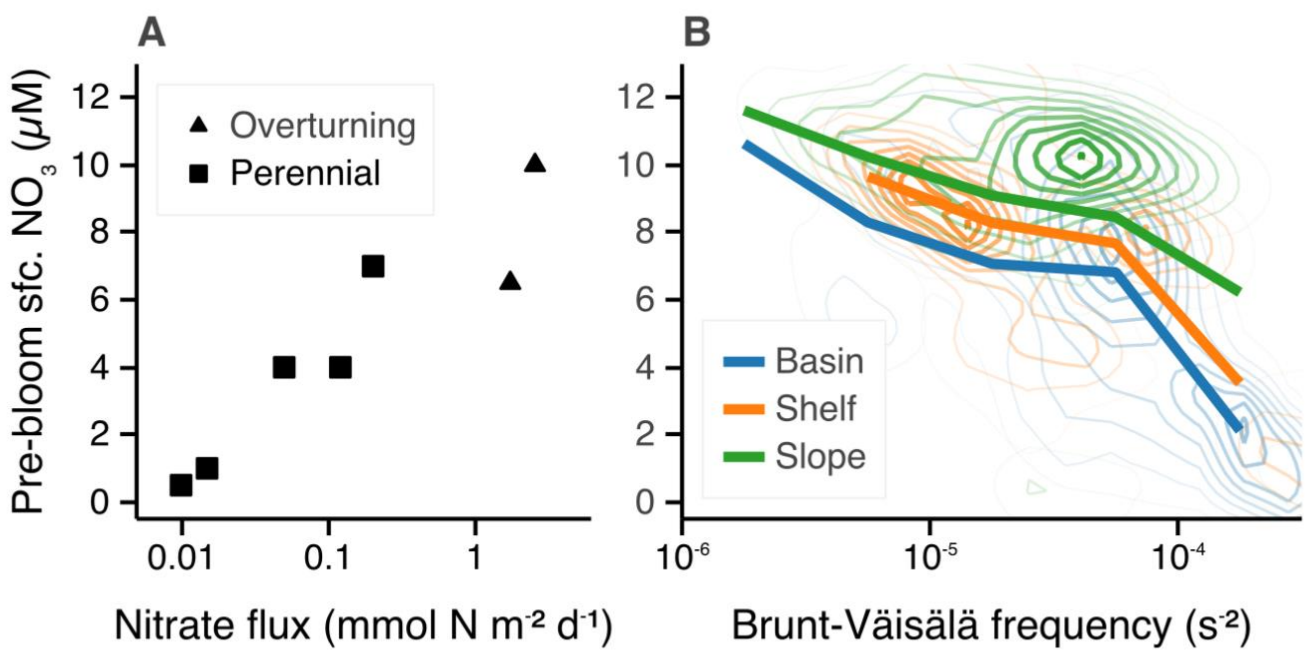

Figure 4: The surface nitrate inventory dominated by variations in turbulent mixing. The annual pre-bloom nitrate inventory graphed as a function of (A) the vertical nitrate flux during winter and (B) the strength of water column stratification in the upper 30-60 m depth interval. The bold curves show average nitrate concentration for a given strength of

stratification for either of three bathymetry types, whereas the closed contours indicate the underlying probability distribution of all data points. Data sources: (A) nitrate flux compilation, (B) nitrate profile database.

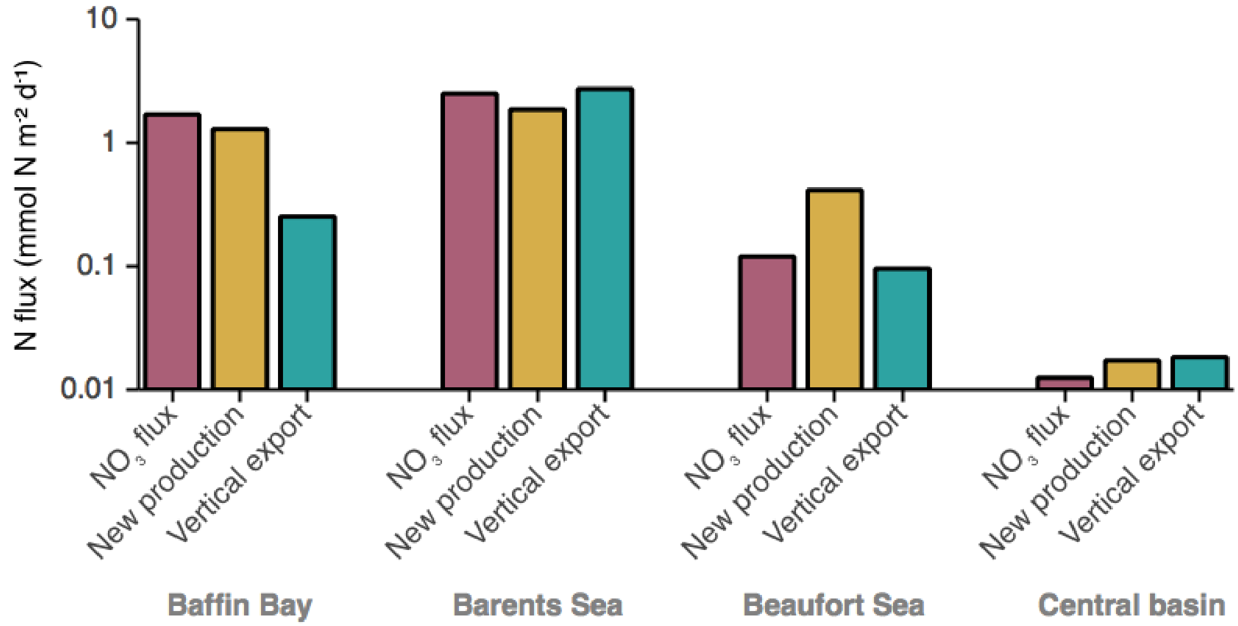

Figure 5: Upward nitrate flux, new production, and vertical downward particle export (Redfield-equivalent) at 200 m depth compared across four regions of the Arctic Ocean. Data sources: Nitrate fluxes, see Table 1; new production, Sakshaug (2004); export production, Wiedmann (2015), Honjo et al. (2010), and Cai et al. (2010)

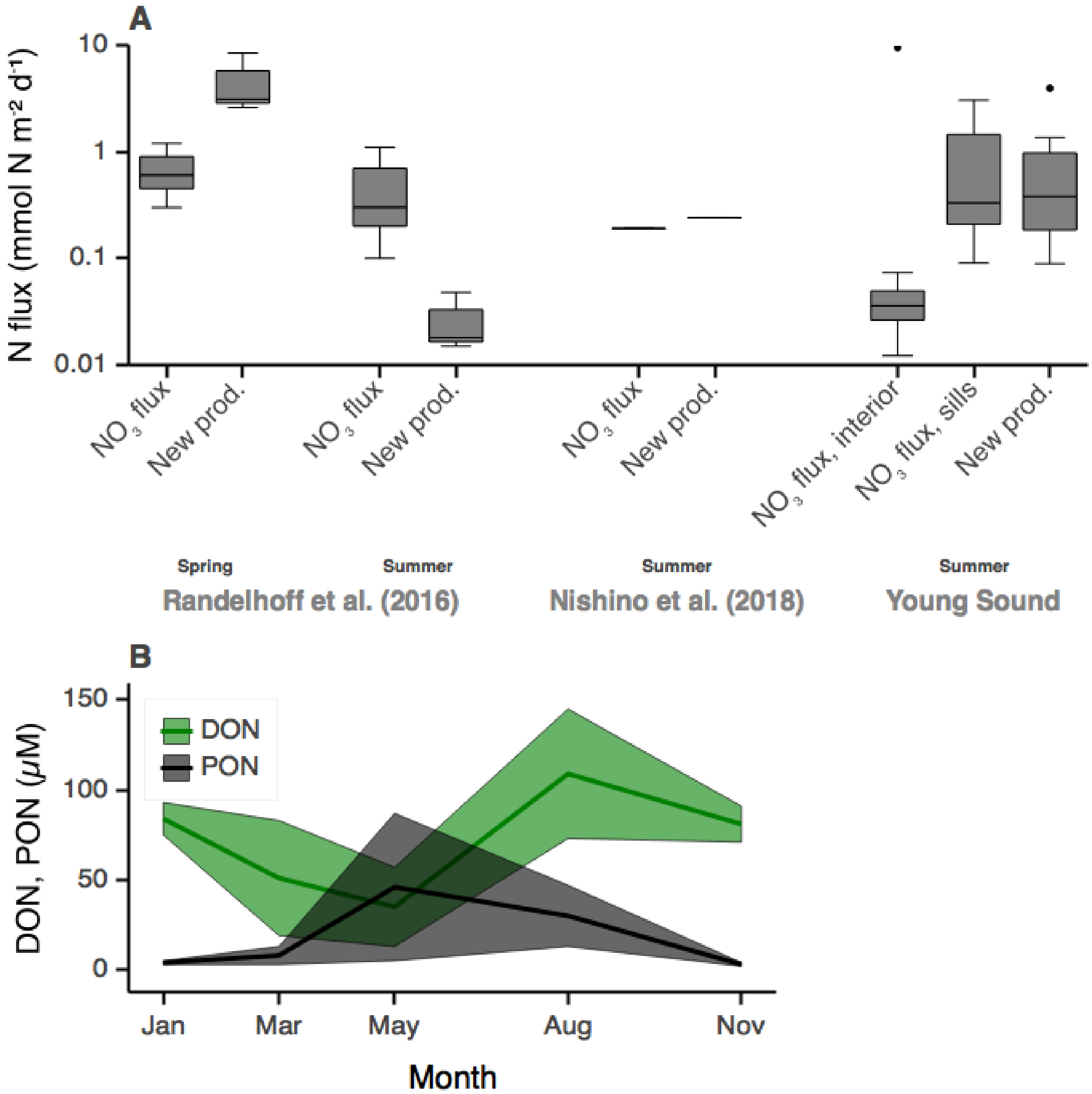

Figure 6: (A) New production incubations compared with upward nitrate flux for three case studies. Data sources: Randelhoff et al. (2016), Nishino et al. (2015), this study (see Appendix). (B) Annual cycle of dissolved (DON) and particulate organic nitrogen (PON) observed in the seasonal ice zone of Fram Strait. Shaded areas indicate the standard deviation. Data source: Paulsen et al. (2018), their Table 1

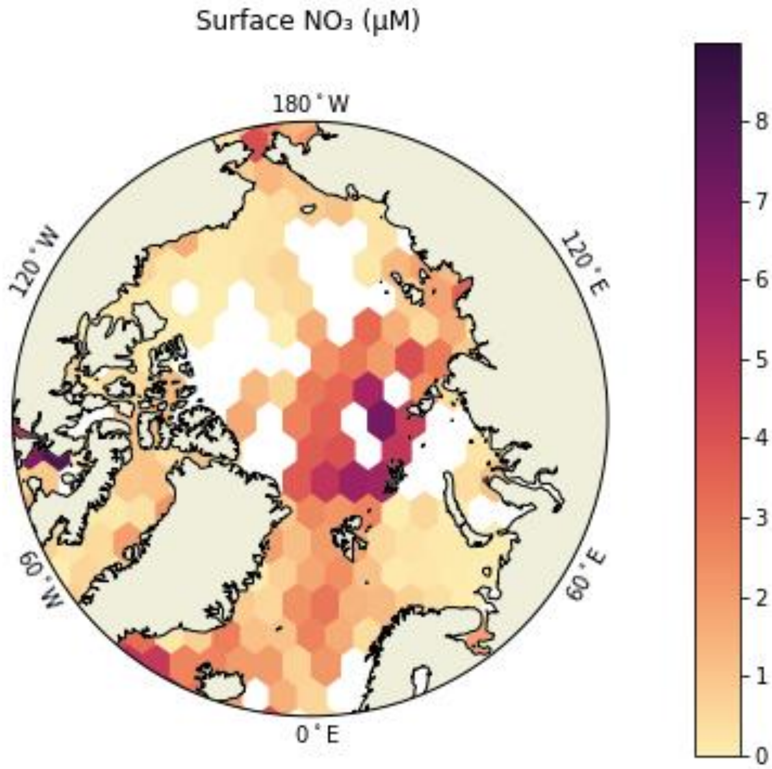

Figure 7: Summer surface nitrate concentration.

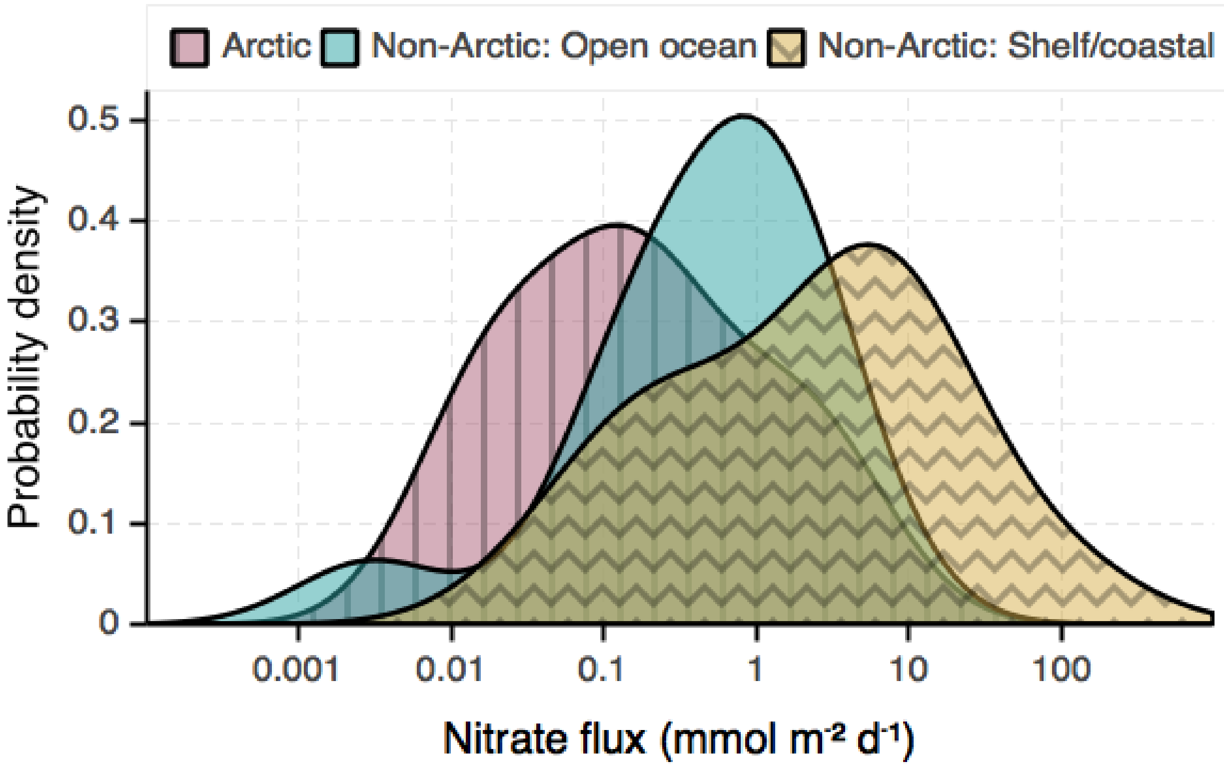

Figure 8: Distributions (kernel density estimates) of observed nitrate fluxes based on Tables 1 and 2. Note that these curves give each observation the same weight, regardless of areal or temporal scope.

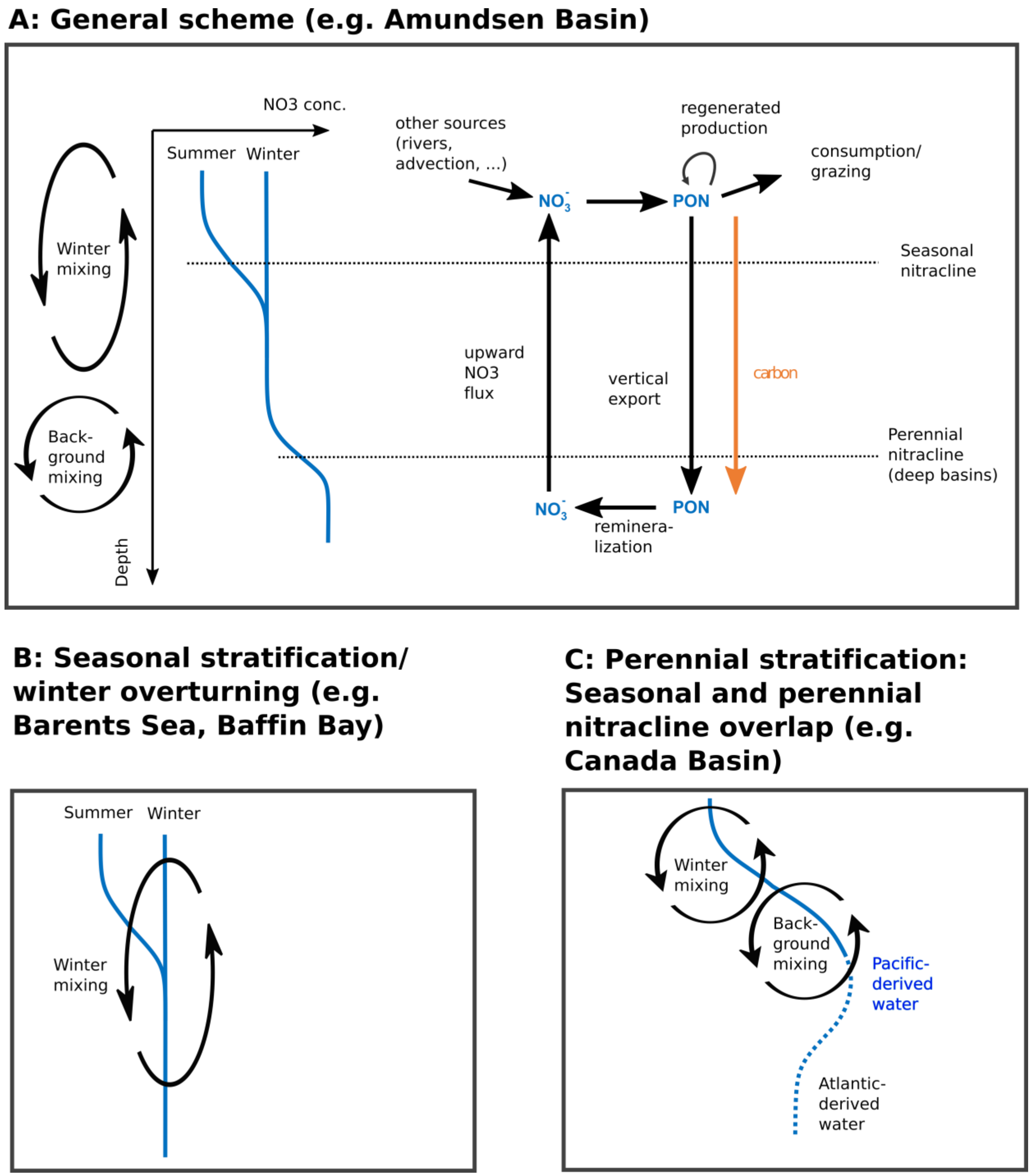

Figure 9: A simplified marine nitrogen cycle and idealized Arctic hydrography. (A) General schematic of a vertical profile of nitrate concentration, along with the respective portion of the nitrogen cycle that takes place in each layer. In this idealized case, there is a clear separation between the seasonal variations in nitrate concentrations in the surface layer which give rise to the seasonal nitracline, and the underlying perennial nitracline. (B) In areas

with deep overturning into the waters of maximum nitrate concentration, the deep nitracline ceases to be meaningful. Instead, nitrate fluxes tap into high-nutrient water every winter. (C) Highly stratified areas do not see large seasonal excursions in surface layer nitrate concentrations or mixing depths.

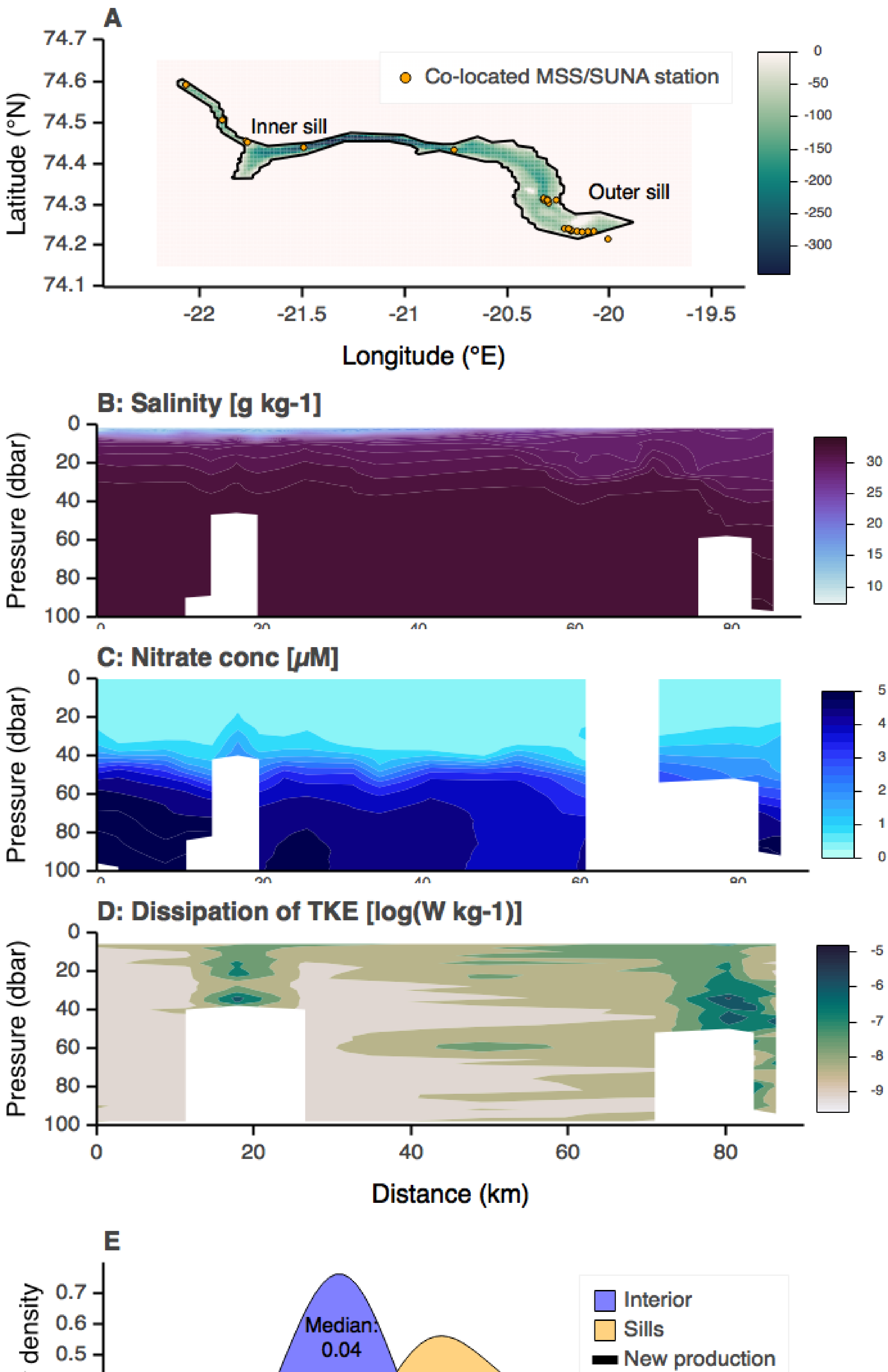
A
Co-located MSS/SUNA station
Inner sill
Outer sill
Latitude (°N)
Longitude (°E)
74.7
74.6
74.5
74.4
74.3
74.2
74.1
-22
-21.5
-21
-20.5
-20
-19.5
0
-50
-100
-150
-200
-250
-300
B: Salinity [g kg-1]
Pressure (dbar)
30
25
20
15
10
C: Nitrate conc [μM]
Pressure (dbar)
5
4
3
2
1
0
D: Dissipation of TKE [log(W kg-1)]
Pressure (dbar)
-5
-6
-7
-8
-9
0
20
40
60
80
100
Distance (km)
E
density
0.7
0.6
0.5
Median:
0.04
Interior
Sills
New production

Figure 10: Young Sound data. (A) Bathymetry and coast data courtesy T. Vang and J. Bendtsen (Rysgaard et al. (2003); not included in the supplemental material). Transect starting in the inner end of the fjord, going over two sills and out into the Greenland Sea, demonstrating (B) low salinity due to ice sheet runoff, (C) nitrate depletion in the upper 30-40 meters, and (D) a quiescent fjord interior with vigorous mixing over the two sills. (E) Upward nitrate fluxes observed in Young Sound (shaded areas represent kernel density estimates) and observed values of integrated new production (black bars). Note that new production estimates are based on only two measurement depths; see methods.

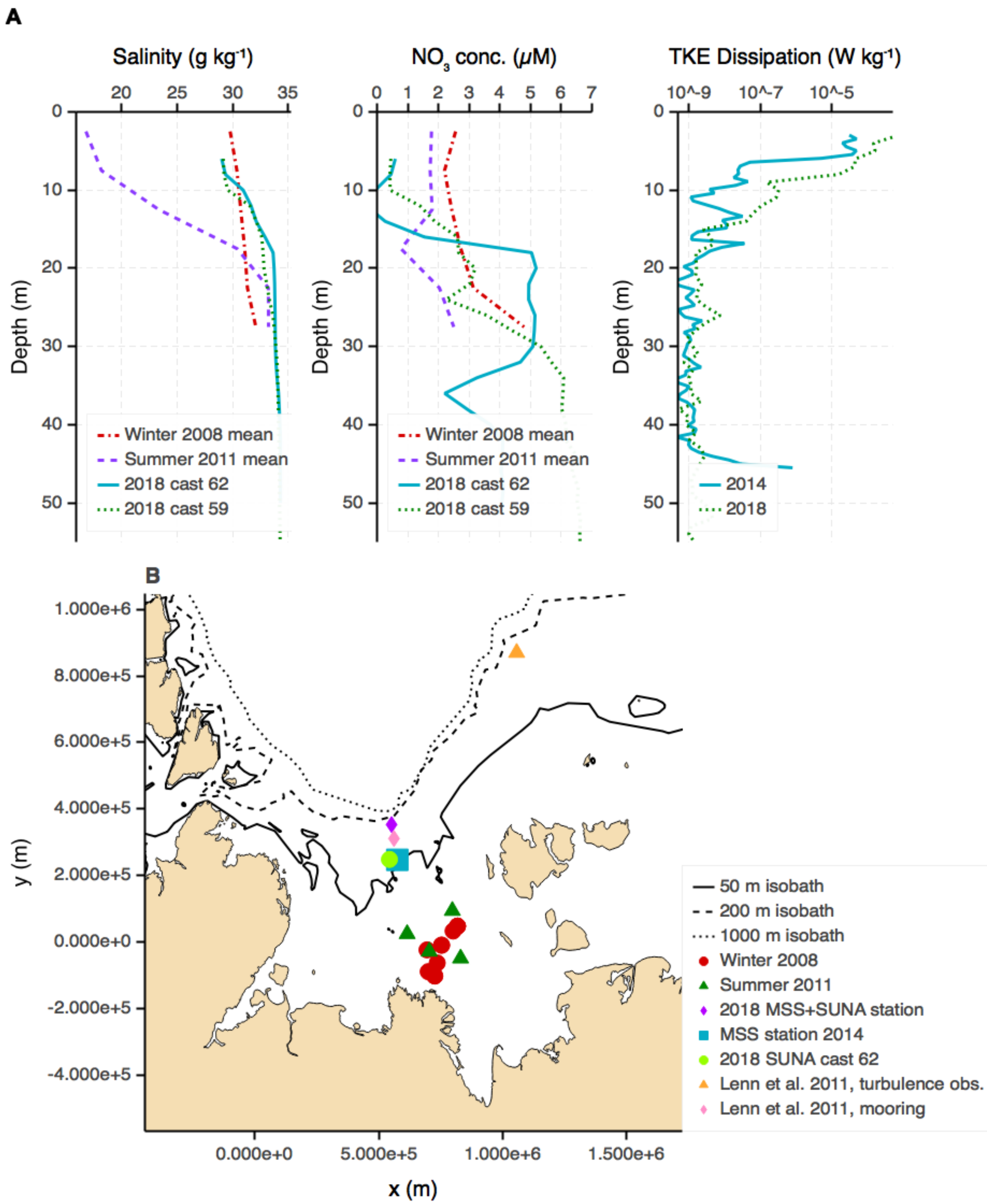

Figure 11: Laptev Sea data. (A) Vertical profiles of salinity, nitrate concentration and dissipation of turbulent kinetic energy (ϵ) in the Laptev Sea. (B) Measurement locations in the Laptev Sea. Map drawn using a Lambert conformal projection (PROJ4 string: `+ellps=WGS84`

+proj=lcc +lon_0=110 +lat_0=75 +x_0=0.0 +y_0=0.0 +lat_1=33 +lat_2=45 +no_defs).

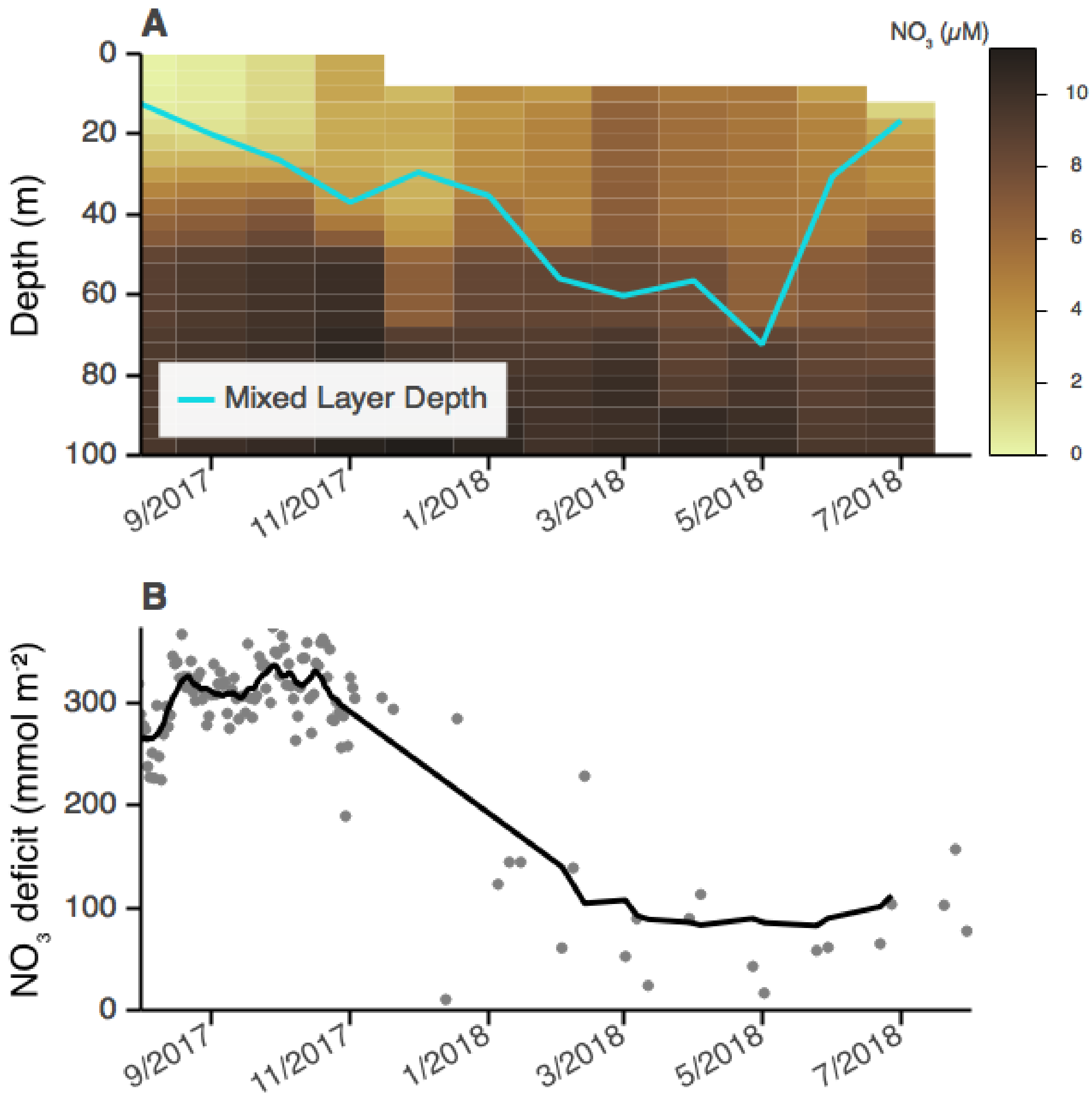

Figure 12: Seasonal cycle of nitrate concentrations in Baffin Bay alongside mixed layer depth (A) and the 0-60 m vertically integrated nitrate deficit $\Delta[NO_3^-] = [NO_3^-](60m) - [NO_3^-](z)$ *(B).*

15 Tables

Table 1: Nitrate fluxes observed in the Arctic Ocean. AABC: Anticyclonic Arctic Boundary Current. Perennial: Measured below the extent of seasonal nitrate variation. See Supplementary Material for complete data set.

Reference	FN	Region	Season	Sample size
Sundfjord et al. (2007)	0.1	Barents Sea	Summer	Few measurements
Sundfjord et al. (2007)	2.0	Barents Sea	Summer	Few measurements
Bourgault et al. (2011)	0.12	Amundsen Gulf	Winter	Aggregate value
Randelhoff et al. (2015)	2.5	Barents Sea, AABC	Winter	Aggregate value
this study, Nishino et al. (2015)	0.02	Chukchi Sea	Summer	Few measurements
Randelhoff and Guthrie (2016)	0.01	Canada Basin	Perennial	Aggregate value
Randelhoff and Guthrie (2016)	0.015	Makarov Basin	Perennial	Aggregate value
Randelhoff and Guthrie (2016)	0.05	Amundsen Basin	Perennial	Aggregate value
Randelhoff and Guthrie (2016)	0.2	Nansen Basin/Yermak Plateau	Perennial	Aggregate value
Randelhoff et al. (2016)	0.3	N Svalbard/Fram Strait	Summer	Aggregate value
Randelhoff et al. (2016)	0.7	N Svalbard/Fram Strait	Summer	Aggregate value
Wiedmann et al. (2017)	0.1	Barents Sea	Summer	Few measurements
Wiedmann et al. (2017)	5.0	Barents Sea	Summer	Few measurements
Nishino et al. (2018)	0.19	Chukchi Sea	Summer	Aggregate value

this study	1.7	Baffin Bay	Winter	Aggregate value
this study	0.015	Laptev Shelf (outer)	Summer	Few measurements
this study	0.33	Young Sound (Sills)	Summer	Aggregate value
this study	0.035	Young Sound (Interior)	Summer	Aggregate value

Table 2: Nitrate fluxes in the global ocean, excluding the Arctic.

Reference	**FN**	**Region**
Lewis et al. (1986)	0.14	Subtropical North Atlantic
Jenkins (1988)	1.6	Subtropical North Atlantic
Hamilton et al. (1989) re-analyzing Lewis et al. (1986)	0.85	Subtropical North Atlantic
Carr et al. (1995)	1.9	Equatorial Pacific (5 °N - 5 °S)
Carr et al. (1995)	4.3	Equatorial Pacific (1 °N - 1 °S)
Horne et al. (1996)	0.047	North Atlantic, Georges Bank
Horne et al. (1996)	0.18	North Atlantic, Georges Bank
Planas et al. (1999)	0.38	Central Atlantic
Law et al. (2001)	1.8	Subarctic North Atlantic
Sharples et al. (2001)	12.0	New Zealand Shelf
Law (2003)	0.17	Antarctic Circumpolar Current
Hales (2005)	9.0	Oregon Shelf Upwelling System
Sharples et al. (2007)	1.3	Celtic Sea shelf edge (neap tide)
Sharples et al. (2007)	9.0	Celtic Sea shelf edge (spring tide)

Hales et al. (2009)	0.9	New England shelf break front (seaward of)
Hales et al. (2009)	5.2	New England shelf break front (shoreward of)
Rippeth et al. (2009)	1.5	Irish Sea
Martin et al. (2010)	0.09	North Atlantic, Porcupine Abyssal Plain
Schafstall et al. (2010)	1.0	Mauritanian Upwelling (offshore)
Schafstall et al. (2010)	3.7	Mauritanian Upwelling (shelf)
Schafstall et al. (2010)	10.0	Mauritanian Upwelling (slope)
Shiozaki et al. (2011), mean of values in their Table 1	0.25	North Pacific, East China Sea shelf
Kaneko et al. (2013)	0.003	North Pacific, Kuroshio (south of front)
Kaneko et al. (2013)	0.34	North Pacific, Kuroshio (north of front)
Cyr et al. (2015)	0.21	St. Lawrence Gulf, Canada
Cyr et al. (2015)	95.0	St. Lawrence Gulf, Canada (shallow sill)

16 References

Aagaard, K., and Carmack, E. C. (1989). The role of sea ice and other fresh water in the Arctic circulation. *Journal of Geophysical Research: Oceans* 94, 14485–14498. doi:10.1029/JC094iC10p14485.

Alkire, M. (2019). Ocean conductivity, temperature, density (CTD), oxygen, and nitrate profiles, Eurasian and Makarov basins, Arctic Ocean, 2013-2018. doi:10.18739/A24X54G9W.

Alkire, M. B., Falkner, K. K., Morison, J., Collier, R. W., Guay, C. K., Desiderio, R. A., et al. (2010). Sensor-based profiles of the NO parameter in the central Arctic and southern Canada Basin New insights regarding the cold halocline. *Deep-Sea Research Part I-Oceanographic Research Papers* 57, 1432–1443. doi:10.1016/j.dsr.2010.07.011.

Allen, T. F. H., and Hoekstra, T. W. (2015). *Toward a unified ecology*. Second edition. New York: Columbia University Press.

Ambühl, H. (1959). Die Bedeutung der Strömung als ökologischer Faktor. *Schweizerische Zeitschrift für Hydrologie* 21, 133. doi:10.1007/BF02505455.

Ardyna, M., Babin, M., Gosselin, M., Devred, E., Rainville, L., and Tremblay, J.-É. (2014). Recent Arctic Ocean sea ice loss triggers novel fall phytoplankton blooms. *Geophysical Research Letters* 41, 6207–6212. doi:10.1002/2014gl061047.

Arrigo, K. R., Mills, M. M., Dijken, G. L. van, Lowry, K. E., Pickart, R. S., and Schlitzer, R. (2017). Late Spring Nitrate Distributions Beneath the Ice-Covered Northeastern Chukchi Shelf. *Journal of Geophysical Research: Biogeosciences* 122, 2409–2417. doi:10.1002/2017JG003881.

Arrigo, K. R., and van Dijken, G. L. (2015). Continued increases in Arctic Ocean primary production. *Progress in Oceanography* 136, 60–70. doi:10.1016/j.pocean.2015.05.002.

Bauch, D., Cherniavskaia, E., Novikhin, A., and Kassens, H. (2018). Physical oceanography, nutrients, and Δ^{18}O measured on water bottle samples in the Laptev Sea, supplement to: Bauch, D; Cherniavskaia, Ekaterina (2018): Water Mass Classification on a Highly Variable Arctic Shelf Region: Origin of Laptev Sea Water Masses and Implications for the Nutrient Budget. Journal of Geophysical Research: Oceans. doi:10.1594/PANGAEA.885448.

Biogeochemical-Argo Planning Group (2016). The scientific rationale, design and implementation plan for a Biogeochemical-Argo float array. Ifremer doi:10.13155/46601.

Blais, M., Tremblay, J.-É., Jungblut, A. D., Gagnon, J., Martin, J., Thaler, M., et al. (2012). Nitrogen fixation and identification of potential diazotrophs in the Canadian Arctic. *Global Biogeochemical Cycles* 26. doi:10.1029/2011gb004096.

Bluhm, B. A., Kosobokova, K. N., and Carmack, E. C. (2015). A tale of two basins: An integrated physical and biological perspective of the deep Arctic Ocean. *Progress in Oceanography* 139, 89–121. doi:10.1016/j.pocean.2015.07.011.

Bokeh Development Team (2018). *Bokeh: Python library for interactive visualization*.

Bouffard, D., and Boegman, L. (2013). A diapycnal diffusivity model for stratified environmental flows. *Dynamics of Atmospheres and Oceans* 61-62, 14–34. doi:10.1016/j.dynatmoce.2013.02.002.

Bouman, H. A., Platt, T., Doblin, M., Figueiras, F. G., Gudmundsson, K., Gudfinnsson, H. G., et al. (2018). PhotosynthesisIrradiance parameters of marine phytoplankton: Synthesis of a global data set. *Earth System Science Data* 10, 251–266. doi:https://doi.org/10.5194/essd-10-251-2018.

Bourgault, D., Hamel, C., Cyr, F., Tremblay, J.-É., Galbraith, P. S., Dumont, D., et al. (2011). Turbulent nitrate fluxes in the Amundsen Gulf during ice-covered conditions. *Geophysical Research Letters* 38. doi:10.1029/2011GL047936.

Brzezinski, M. A. (1985). The Si:C:N ratio of marine diatoms: Interspecific variability and the effect of some environmental variables. *Journal of Phycology* 21, 347–357.

Cai, P., Rutgers van der Loeff, M., Stimac, I., NÃthig, E.-M., Lepore, K., and Moran, S. B. (2010). Low export flux of particulate organic carbon in the central Arctic Ocean as revealed by 234Th:238U disequilibrium. *Journal of Geophysical Research: Oceans* 115, n/a–n/a. doi:10.1029/2009JC005595.

Carmack, E., Barber, D., Christensen, J., Macdonald, R., Rudels, B., and Sakshaug, E. (2006). Climate variability and physical forcing of the food webs and the carbon budget on panarctic shelves. *Progress in Oceanography* 71, 145–181. doi:10.1016/j.pocean.2006.10.005.

Carmack, E. C. (2007). The alpha/beta ocean distinction: A perspective on freshwater fluxes, convection, nutrients and productivity in high-latitude seas. *Deep Sea Research Part II: Topical Studies in Oceanography* 54, 2578–2598. doi:10.1016/j.dsr2.2007.08.018.

Carmack, E., and Chapman, D. C. (2003). Wind-driven shelf/basin exchange on an Arctic shelf: The joint roles of ice cover extent and shelf-break bathymetry. *Geophys. Res. Lett.* 30. doi:10.1029/2003gl017526.

Carmack, E., and Wassmann, P. (2006). Food webs and physical - biological coupling on pan-Arctic shelves: Unifying concepts and comprehensive perspectives. *Progress in Oceanography* 71, 446–477. doi:10.1016/j.pocean.2006.10.004.

Carr, M.-E., Lewis, M. R., Kelley, D., and Jones, B. (1995). A physical estimate of new production in the equatorial Pacific along 150W. *Limnology and Oceanography* 40, 138–147. doi:10.4319/lo.1995.40.1.0138.

Chanona, M., Waterman, S., and Gratton, Y. (2018). Variability of Internal Wave-Driven Mixing and Stratification in Canadian Arctic Shelf and Shelf-Slope Waters. *Journal of Geophysical Research: Oceans* 123, 9178–9195. doi:10.1029/2018JC014342.

Codispoti, L. A., Kelly, V., Thessen, A., Matrai, P., Suttles, S., Hill, V., et al. (2013). Synthesis of primary production in the Arctic Ocean: III. Nitrate and phosphate based estimates of net community production. *Progress in Oceanography* 110, 126–150. doi:10.1016/j.pocean.2012.11.006.

Cole, S. T., Toole, J. M., Rainville, L., and Lee, C. M. (2018). Internal waves in the Arctic: Influence of ice concentration, ice roughness, and surface layer stratification. *Journal of Geophysical Research: Oceans*. doi:10.1029/2018JC014096.

Collos, Y. (1987). Calculations of 15N uptake rates by phytoplankton assimilating one or several nitrogen sources. *International Journal of Radiation Applications and Instrumentation. Part A. Applied Radiation and Isotopes* 38, 275–282. doi:10.1016/0883-2889(87)90038-4.

Comiso, J. C. (2012). Large decadal decline of the Arctic multiyear ice cover. *Journal of Climate* 25, 1176–1193. doi:10.1175/JCLI-D-11-00113.1.

Crews, L., Sundfjord, A., Albretsen, J., and Hattermann, T. (2018). Mesoscale Eddy Activity and Transport in the Atlantic Water Inflow Region North of Svalbard. *Journal of Geophysical Research: Oceans* 123, 201–215. doi:10.1002/2017JC013198.

Cyr, F., Bourgault, D., Galbraith, P. S., and Gosselin, M. (2015). Turbulent nitrate fluxes in the Lower St. Lawrence Estuary (Canada). *J. Geophys. Res. Oceans*, n/a–n/a. doi:10.1002/2014jc010272.

Dewey, S. R., Morison, J. H., and Zhang, J. (2017). An Edge-Referenced Surface Fresh Layer in the Beaufort Sea Seasonal Ice Zone. *Journal of Physical Oceanography* 47, 1125–1144. doi:10.1175/JPO-D-16-0158.1.

Dosser, H. V., and Rainville, L. (2016). Dynamics of the Changing Near-Inertial Internal Wave Field in the Arctic Ocean. *Journal of Physical Oceanography* 46, 395–415. doi:10.1175/jpo-d-15-0056.1.

Dugdale, R. C., and Goering, J. J. (1967). Uptake of new and regenerated forms of nitrogen in primary productivity. *Limnology and Oceanography* 12, 196–206. doi:10.4319/lo.1967.12.2.0196.

Eppley, R., and Peterson, B. (1979). The flux of particulate organic matter to the deep ocean and its relation to planktonic new production. *Nature* 282, 677–680.

Fer, I., and Drinkwater, K. (2014). Mixing in the Barents Sea Polar Front near Hopen in spring. *Journal of Marine Systems* 130, 206–218. doi:10.1016/j.jmarsys.2012.01.005.

Frey, K. E., and McClelland, J. W. (2009). Impacts of permafrost degradation on arctic river biogeochemistry. *Hydrological Processes* 23, 169–182. doi:10.1002/hyp.7196.

Frigstad, H., Andersen, T., Bellerby, R. G. J., Silyakova, A., and Hessen, D. O. (2014). Variation in the seston C:N ratio of the Arctic Ocean and pan-Arctic shelves. *Journal of Marine Systems* 129, 214–223. doi:10.1016/j.jmarsys.2013.06.004.

Gargett, A., and Garner, T. (2008). Determining Thorpe Scales from Ship-Lowered CTD Density Profiles. *Journal of Atmospheric and Oceanic Technology* 25, 1657–1670. doi:10.1175/2008jtecho541.1.

Garrett, C., and Munk, W. (1975). Space-time scales of internal waves: A progress report. *Journal of Geophysical Research* 80, 291–297. doi:10.1029/JC080i003p00291.

Gregg, M. C., D'Asaro, E. A., Riley, J. J., and Kunze, E. (2018). Mixing Efficiency in the Ocean. *Annual Review of Marine Science* 10, 443–473. doi:10.1146/annurev-marine-121916-063643.

Guthrie, J. D., Morison, J. H., and Fer, I. (2013). Revisiting internal waves and mixing in the Arctic Ocean. *Journal of Geophysical Research: Oceans* 118, 3966–3977. doi:10.1002/jgrc.20294.

Hales, B. (2005). Irreversible nitrate fluxes due to turbulent mixing in a coastal upwelling system. *Journal of Geophysical Research* 110, C10S11. doi:10.1029/2004JC002685.

Hales, B., Hebert, D., and Marra, J. (2009). Turbulent supply of nutrients to phytoplankton at the New England shelf break front. *Journal of Geophysical Research* 114, C05010. doi:10.1029/2008JC005011.

Hamilton, J. M., Lewis, M. R., and Ruddick, B. R. (1989). Vertical fluxes of nitrate associated with salt fingers in the world's oceans. *Journal of Geophysical Research: Oceans* 94, 2137–2145. doi:10.1029/JC094iC02p02137.

Hattermann, T., Isachsen, P. E., von Appen, W.-J., Albretsen, J., and Sundfjord, A. (2016). Eddy-driven recirculation of Atlantic Water in Fram Strait. *Geophysical Research Letters* 43, 3406–3414. doi:10.1002/2016gl068323.

Holding, J. M., Markager, S., Juul-Pedersen, T., Paulsen, M. L., Møller, E. F., Meire, L., et al. (2019). Seasonal and spatial patterns of primary production in a high-latitude fjord affected by Greenland Ice Sheet run-off. *Biogeosciences* 16, 3777–3792. doi:https://doi.org/10.5194/bg-16-3777-2019.

Honjo, S., Krishfield, R. A., Eglinton, T. I., Manganini, S. J., Kemp, J. N., Doherty, K., et al. (2010). Biological pump processes in the cryopelagic and hemipelagic Arctic Ocean: Canada Basin and Chukchi Rise. *Progress in Oceanography* 85, 137–170. doi:http://dx.doi.org/10.1016/j.pocean.2010.02.009.

Hopwood, M. J., Carroll, D., Browning, T., Meire, L., Mortensen, J., Krisch, S., et al. (2018). Non-linear response of summertime marine productivity to increased meltwater discharge around Greenland. *Nature communications* 9, 3256.

Hopwood, M. J., Carroll, D., Dunse, T., Hodson, A., Holding, J. M., Iriarte, J. L., et al. (2019). How does glacier discharge affect marine biogeochemistry and primary production in the Arctic? *The Cryosphere Discussions*, 1–51.

Horne, E. P. W., Loder, J. W., Naime, C. E., and Oakey, N. S. (1996). Turbulence dissipation rates and nitrate supply in the upper water column on Georges Bank. *Deep Sea Research Part II: Topical Studies in Oceanography* 43, 1683–1712. doi:10.1016/S0967-0645(96)00037-9.

Ivanov, V., Alexeev, V., Koldunov, N. V., Repina, I., Sandø, A. B., Smedsrud, L. H., et al. (2016). Arctic Ocean heat impact on regional ice decay - a suggested positive feedback. *Journal of Physical Oceanography* 46, 1437–1456. doi:10.1175/jpo-d-15-0144.1.

Jenkins, W. J. (1988). Nitrate flux into the euphotic zone near Bermuda. *Nature* 331, 521–523. doi:10.1038/331521a0.

Johnson, K. S., Riser, S. C., and Karl, D. M. (2010). Nitrate supply from deep to near-surface waters of the North Pacific subtropical gyre. *Nature* 465, 1062–1065. doi:10.1038/nature09170.

Kalvelage, T., Jensen, M. M., Contreras, S., Revsbech, N. P., Lam, P., Günter, M., et al. (2011). Oxygen sensitivity of anammox and coupled N-cycle processes in oxygen minimum zones. *PloS one* 6, e29299.

Kaneko, H., Yasuda, I., Komatsu, K., and Itoh, S. (2013). Observations of vertical turbulent nitrate flux across the Kuroshio. *Geophysical Research Letters* 40, 3123–3127. doi:10.1002/grl.50613.

Kämpf, J., and Chapman, P. (2016). *Upwelling Systems of the World*. Springer.

Kowalik, Z., and Proshutinsky, A. Y. (2013). "The Arctic Ocean Tides," in *The Polar Oceans and Their Role in Shaping the Global Environment* (American Geophysical Union (AGU)), 137–158. doi:10.1029/GM085p0137.

Law, C. S. (2003). Vertical eddy diffusion and nutrient supply to the surface mixed layer of the Antarctic Circumpolar Current. *Journal of Geophysical Research* 108, 3272. doi:10.1029/2002JC001604.

Law, C. S., Martin, A. P., Liddicoat, M. I., Watson, A. J., Richards, K. J., and Woodward, E. M. S. (2001). A Lagrangian SF6 tracer study of an anticyclonic eddy in the North Atlantic: Patch evolution, vertical mixing and nutrient supply to the mixed layer. *Deep Sea Research Part II: Topical Studies in Oceanography* 48, 705–724. doi:10.1016/S0967-0645(00)00112-0.

Lewis, M. R., Hebert, D., Harrison, W. G., Platt, T., and Oakey, N. S. (1986). Vertical Nitrate Fluxes in the Oligotrophic Ocean. *Science* 234, 870–873. doi:10.1126/science.234.4778.870.

Li, W. K. W., McLaughlin, F. A., Lovejoy, C., and Carmack, E. C. (2009). Smallest Algae Thrive As the Arctic Ocean Freshens. *Science* 326, 539–539. doi:10.1126/science.1179798.

Lincoln, B. J., Rippeth, T. P., Lenn, Y.-D., Timmermans, M. L., Williams, W. J., and Bacon, S. (2016). Wind-driven mixing at intermediate depths in an ice-free Arctic Ocean. *Geophysical Research Letters* 43, 9749–9756. doi:10.1002/2016GL070454.

Lueck, R. G., Wolk, F., and Yamazaki, H. (2002). Oceanic Velocity Microstructure Measurements in the 20th Century. *Journal of Oceanography* 58, 153–174. doi:10.1023/A:1015837020019.

Margalef, R. (1978). Life-forms of phytoplankton as survival alternatives in an unstable environment. *Oceanologica acta* 1, 493–509.

Martin, A. P., Lucas, M. I., Painter, S. C., Pidcock, R., Prandke, H., Prandke, H., et al. (2010). The supply of nutrients due to vertical turbulent mixing: A study at the Porcupine Abyssal Plain study site in the northeast Atlantic. *Deep Sea Research Part II: Topical Studies in Oceanography* 57, 1293–1302. doi:10.1016/j.dsr2.2010.01.006.

Martin, A. P., and Pondaven, P. (2003). On estimates for the vertical nitrate flux due to eddy pumping. *Journal of Geophysical Research: Oceans* 108, n/a–n/a. doi:10.1029/2003JC001841.

Martin, A. P., and Richards, K. J. (2001). Mechanisms for vertical nutrient transport within a North Atlantic mesoscale eddy. *Deep Sea Research Part II: Topical Studies in Oceanography* 48, 757–773. doi:10.1016/S0967-0645(00)00096-5.

Martin, T., Tsamados, M., Schroeder, D., and Feltham, D. L. (2016). The impact of variable sea ice roughness on changes in Arctic Ocean surface stress: A model study. *Journal of Geophysical Research: Oceans* 121, 1931–1952. doi:10.1002/2015JC011186.

McPhee, M. G. (1992). Turbulent heat flux in the upper ocean under sea ice. *Journal of Geophysical Research: Oceans* 97, 5365–5379. doi:10.1029/92JC00239.

McPhee, M. G., and Kantha, L. H. (1989). Generation of internal waves by sea ice. *Journal of Geophysical Research: Oceans* 94, 3287–3302. doi:10.1029/JC094iC03p03287.

Moore, C. M., Mills, M. M., Arrigo, K. R., Berman-Frank, I., Bopp, L., Boyd, P. W., et al. (2013). Processes and patterns of oceanic nutrient limitation. *Nature Geoscience* 6, 701–710. doi:10.1038/ngeo1765.

Moran, S. B., Weinstein, S. E., Edmonds, H. N., Smith, J. N., Kelly, R. P., Pilson, M. E. Q., et al. (2003). Does 234Th/238U disequilibrium provide an accurate record of the export flux of particulate organic carbon from the upper ocean? *Limnology and Oceanography* 48, 1018–1029. doi:10.4319/lo.2003.48.3.1018.

Moum, J. N., Gregg, M. C., Lien, R. C., and Carr, M. E. (1995). Comparison of Turbulence Kinetic Energy Dissipation Rate Estimates from Two Ocean Microstructure Profilers.

Journal of Atmospheric and Oceanic Technology 12, 346–366. doi:10.1175/1520-0426(1995)012<0346:COTKED>2.0.CO;2.

Nishino, S., Kawaguchi, Y., Fujiwara, A., Shiozaki, T., Aoyama, M., Harada, N., et al. (2018). Biogeochemical Anatomy of a Cyclonic Warm-Core Eddy in the Arctic Ocean. *Geophysical Research Letters* 0. doi:10.1029/2018GL079659.

Nishino, S., Kawaguchi, Y., Inoue, J., Hirawake, T., Fujiwara, A., Futsuki, R., et al. (2015). Nutrient supply and biological response to wind-induced mixing, inertial motion, internal waves, and currents in the northern Chukchi Sea. *Journal of Geophysical Research: Oceans* 120, 1975–1992. doi:10.1002/2014jc010407.

Nummelin, A., Ilicak, M., Li, C., and Smedsrud, L. H. (2015). Consequences of future increased Arctic runoff on Arctic Ocean stratification, circulation, and sea ice cover. *Journal of Geophysical Research: Oceans*. doi:10.1002/2015jc011156.

Omand, M. M., Feddersen, F., Guza, R. T., and Franks, P. J. S. (2012). Episodic vertical nutrient fluxes and nearshore phytoplankton blooms in Southern California. *Limnology and Oceanography* 57, 1673–1688. doi:10.4319/lo.2012.57.6.1673.

Onarheim, I. H., Eldevik, T., Smedsrud, L. H., and Stroeve, J. C. (2018). Seasonal and Regional Manifestation of Arctic Sea Ice Loss. *Journal of Climate* 31, 4917–4932. doi:10.1175/JCLI-D-17-0427.1.

Osborn, T. R. (1980). Estimates of the Local Rate of Vertical Diffusion from Dissipation Measurements. *J. Phys. Oceanogr.* 10, 83–89. doi:10.1175/1520-0485(1980)010<0083:EOTLRO>2.0.CO;2.

Paulsen, M. L., Nielsen, S. E. B., Müller, O., Møller, E. F., Stedmon, C. A., Juul-Pedersen, T., et al. (2017). Carbon Bioavailability in a High Arctic Fjord Influenced by Glacial Meltwater, NE Greenland. *Frontiers in Marine Science* 4. doi:10.3389/fmars.2017.00176.

Paulsen, M. L., Seuthe, L., Reigstad, M., Larsen, A., Cape, M. R., and Vernet, M. (2018). Asynchronous Accumulation of Organic Carbon and Nitrogen in the Atlantic Gateway to the Arctic Ocean. *Frontiers in Marine Science* 5. doi:10.3389/fmars.2018.00416.

Peralta-Ferriz, C., and Woodgate, R. A. (2015). Seasonal and interannual variability of pan-Arctic surface mixed layer properties from 1979 to 2012 from hydrographic data, and the dominance of stratification for multiyear mixed layer depth shoaling. *Progress in Oceanography* 134, 19–53. doi:http://dx.doi.org/10.1016/j.pocean.2014.12.005.

Planas, D., Agustí, S., Duarte, C. M., Granata, T. C., and Merino, M. (1999). Nitrate uptake and diffusive nitrate supply in the Central Atlantic. *Limnology and Oceanography* 44, 116–126. doi:10.4319/lo.1999.44.1.0116.

Polyakov, I. V., Pnyushkov, A. V., Alkire, M. B., Ashik, I. M., Baumann, T. M., Carmack, E. C., et al. (2017). Greater role for Atlantic inflows on sea-ice loss in the Eurasian Basin of the Arctic Ocean. *Science* 356, 285–291. doi:10.1126/science.aai8204.

Polzin, K. L., Naveira Garabato, A. C., Huussen, T. N., Sloyan, B. M., and Waterman, S. (2014). Finescale parameterizations of turbulent dissipation. *J. Geophys. Res. Oceans* 119, 1383–1419. doi:10.1002/2013jc008979.

Rainville, L., and Woodgate, R. A. (2009). Observations of internal wave generation in the seasonally ice-free Arctic. *Geophysical Research Letters* 36. doi:10.1029/2009GL041291.

Randelhoff, A., Fer, I., and Sundfjord, A. (2017). Turbulent Upper-Ocean Mixing Affected by Meltwater Layers during Arctic Summer. *Journal of Physical Oceanography* 47, 835–853. doi:10.1175/JPO-D-16-0200.1.

Randelhoff, A., Fer, I., Sundfjord, A., Tremblay, J.-E., and Reigstad, M. (2016). Vertical fluxes of nitrate in the seasonal nitracline of the Atlantic sector of the Arctic Ocean. *Journal of Geophysical Research-Oceans* 121, 5282–5295. doi:10.1002/2016JC011779.

Randelhoff, A., and Guthrie, J. D. (2016). Regional Patterns in Current and Future Export Production in the Central Arctic Ocean Quantified from Nitrate Fluxes. *Geophysical Research Letters*. doi:10.1002/2016gl070252.

Randelhoff, A., Reigstad, M., Chierici, M., Sundfjord, A., Ivanov, V., Cape, M., et al. (2018). Seasonality of the Physical and Biogeochemical Hydrography in the Inflow to the Arctic Ocean Through Fram Strait. *Frontiers in Marine Science* 5. doi:10.3389/fmars.2018.00224.

Randelhoff, A., and Sundfjord, A. (2018). Short commentary on marine productivity at Arctic shelf breaks: Upwelling, advection and vertical mixing. *Ocean Science* 14, 293–300. doi:10.5194/os-14-293-2018.

Randelhoff, A., Sundfjord, A., and Reigstad, M. (2015). Seasonal variability and fluxes of nitrate in the surface waters over the Arctic shelf slope. *Geophysical Research Letters* 42, 3442–3449. doi:10.1002/2015gl063655.

Redfield, A. C., Ketchum, B. H., and Richards, F. A. (1963). "The influence of organisms on the composition of sea-water," in *The Sea*, ed. M. N. Hill (Academic Press), 26–77.

Rees, A. P., Joint, I., Woodward, E. M. S., and Donald, K. M. (2001). Carbon, nitrogen and phosphorus budgets within a mesoscale eddy: Comparison of mass balance with in vitro determinations. *Deep Sea Research Part II: Topical Studies in Oceanography* 48, 859–872. doi:10.1016/S0967-0645(00)00101-6.

Renaud, P. E., Sejr, M. K., Bluhm, B. A., Sirenko, B., and Ellingsen, I. H. (2015). The future of Arctic benthos: Expansion, invasion, and biodiversity. *Progress in Oceanography* 139, 244–257. doi:10.1016/j.pocean.2015.07.007.

Rippeth, T. P., Lincoln, B. J., Lenn, Y.-D., Green, J. A. M., Sundfjord, A., and Bacon, S. (2015). Tide-mediated warming of Arctic halocline by Atlantic heat fluxes over rough topography. *Nature Geoscience* 8, 191–194. doi:10.1038/ngeo2350.

Rippeth, T. P., Wiles, P., Palmer, M. R., Sharples, J., and Tweddle, J. (2009). The diapcynal nutrient flux and shear-induced diapcynal mixing in the seasonally stratified western Irish Sea. *Continental Shelf Research* 29, 1580–1587. doi:10.1016/j.csr.2009.04.009.

Risgaard-Petersen, N., Revsbech, N. P., and Rysgaard, S. (1995). Combined microdiffusion-hypobromite oxidation method for determining nitrogen-15 isotope in ammonium. *Soil Science Society of America Journal* 59, 1077–1080.

Rysgaard, S., Vang, T., Stjernholm, M., Rasmussen, B., Windelin, A., and Kiilsholm, S. (2003). Physical Conditions, Carbon Transport, and Climate Change Impacts in a Northeast

Greenland Fjord. *Arctic, Antarctic, and Alpine Research* 35, 301–312. doi:10.1657/1523-0430(2003)035[0301:PCCTAC]2.0.CO;2.

Sakamoto, C. M., Johnson, K. S., and Coletti, L. J. (2009). Improved algorithm for the computation of nitrate concentrations in seawater using an in situ ultraviolet spectrophotometer. *Limnology and Oceanography: Methods* 7, {132–143}.

Sakshaug, E. (2004). "Primary and Secondary Production in the Arctic Seas," in *The Organic Carbon Cycle in the Arctic Ocean*, eds. R. Stein and R. W. Macdonald (Springer Berlin Heidelberg), 57–81. doi:10.1007/978-3-642-18912-8_3.

Schafstall, J., Dengler, M., Brandt, P., and Bange, H. (2010). Tidal-induced mixing and diapycnal nutrient fluxes in the Mauritanian upwelling region. *Journal of Geophysical Research* 115, C10014. doi:10.1029/2009JC005940.

Scheifele, B., Waterman, S., Merckelbach, L., and Carpenter, J. R. (2018). Measuring the Dissipation Rate of Turbulent Kinetic Energy in Strongly Stratified, Low-Energy Environments: A Case Study From the Arctic Ocean. *Journal of Geophysical Research: Oceans* 123, 5459–5480. doi:10.1029/2017JC013731.

Schnetger, B., and Lehners, C. (2014). Determination of nitrate plus nitrite in small volume marine water samples using vanadium (III) chloride as a reduction agent. *Marine Chemistry* 160, 91–98.

Sharples, J., Moore, C. M., and Abraham, E. R. (2001). Internal tide dissipation, mixing, and vertical nitrate flux at the shelf edge of NE New Zealand. *Journal of Geophysical Research: Oceans* 106, 14069–14081. doi:10.1029/2000JC000604.

Sharples, J., Tweddle, J. F., Green, J. A. M., Palmer, M. R., Kim, Y.-N., Hickman, A. E., et al. (2007). Spring-neap modulation of internal tide mixing and vertical nitrate fluxes at a shelf edge in summer. *Limnology and Oceanography* 52, 1735–1747. doi:10.4319/lo.2007.52.5.1735.

Shih, L. H., Koseff, J. R., Ivey, G. N., and Ferziger, J. H. (2005). Parameterization of turbulent fluxes and scales using homogeneous sheared stably stratified turbulence simulations. *Journal of Fluid Mechanics* 525, 193–214. doi:10.1017/S0022112004002587.

Shiozaki, T., Furuya, K., Kodama, T., and Takeda, S. (2009). Contribution of N2 fixation to new production in the western North Pacific Ocean along 155E. *Marine Ecology Progress Series* 377, 19–32. doi:10.3354/meps07837.

Shiozaki, T., Furuya, K., Kurotori, H., Kodama, T., Takeda, S., Endoh, T., et al. (2011). Imbalance between vertical nitrate flux and nitrate assimilation on a continental shelf: Implications of nitrification. *Journal of Geophysical Research: Oceans* 116. doi:10.1029/2010JC006934.

Spall, M. A., Pickart, R. S., Brugler, E. T., Moore, G. W. K., Thomas, L., and Arrigo, K. R. (2014). Role of shelfbreak upwelling in the formation of a massive under-ice bloom in the Chukchi Sea. *Deep Sea Research Part II: Topical Studies in Oceanography* 105, 17–29. doi:http://dx.doi.org/10.1016/j.dsr2.2014.03.017.

Stein, R., and MacDonald, R. W. eds. (2004). *The Organic Carbon Cycle in the Arctic Ocean*. Springer Science + Business Media doi:10.1007/978-3-642-18912-8.

Stevens, J.-L. R., Rudiger, P., and Bednar, J. A. (2015). HoloViews: Building Complex Visualizations Easily for Reproducible Science. in *Proceedings of the 14th Python in Science Conference*.

Sundfjord, A., Fer, I., Kasajima, Y., and Svendsen, H. (2007). Observations of turbulent mixing and hydrography in the marginal ice zone of the Barents Sea. *Journal of Geophysical Research: Oceans* 112. doi:10.1029/2006JC003524.

Tamelander, T., Reigstad, M., Olli, K., Slagstad, D., and Wassmann, P. (2013). New Production Regulates Export Stoichiometry in the Ocean. *PLoS ONE* 8, e54027. doi:10.1371/journal.pone.0054027.

Tank, S. E., Manizza, M., Holmes, R. M., McClelland, J. W., and Peterson, B. J. (2012). The Processing and Impact of Dissolved Riverine Nitrogen in the Arctic Ocean. *Estuaries and Coasts* 35, 401–415. doi:10.1007/s12237-011-9417-3.

Torres-Valdés, S., Tsubouchi, T., Bacon, S., Naveira-Garabato, A. C., Sanders, R., McLaughlin, F. A., et al. (2013). Export of nutrients from the Arctic Ocean. *J. Geophys. Res. Oceans* 118, 1625–1644. doi:10.1002/jgrc.20063.

Tremblay, J.-E., Anderson, L. G., Matrai, P., Coupel, P., Belanger, S., Michel, C., et al. (2015). Global and regional drivers of nutrient supply, primary production and CO2 drawdown in the changing Arctic Ocean. *Progress in Oceanography* 139, 171–196. doi:10.1016/j.pocean.2015.08.009.

Valiela, I. (2015). *Marine ecological processes*. 3rd ed. Springer-Verlag New York.

Vancoppenolle, M., Bopp, L., Madec, G., Dunne, J., Ilyina, T., Halloran, P. R., et al. (2013). Future Arctic Ocean primary productivity from CMIP5 simulations: Uncertain outcome, but consistent mechanisms. *Global Biogeochemical Cycles* 27, 605–619. doi:10.1002/gbc.20055.

Wassmann, P., Slagstad, D., Riser, C. W., and Reigstad, M. (2006). Modelling the ecosystem dynamics of the Barents Sea including the marginal ice zone. *Journal of Marine Systems* 59, 1–24. doi:10.1016/j.jmarsys.2005.05.006.

Watanabe, E., Onodera, J., Harada, N., Honda, M. C., Kimoto, K., Kikuchi, T., et al. (2014). Enhanced role of eddies in the Arctic marine biological pump. *Nature Communications* 5. doi:10.1038/ncomms4950.

Wiedmann, I. (2015). Potential drivers of the downward carbon and particle flux in Arctic marine ecosystems under contrasting hydrographical and ecological situations.

Wiedmann, I., Tremblay, J.-É., Sundfjord, A., and Reigstad, M. (2017). Upward nitrate flux and downward particulate organic carbon flux under contrasting situations of stratification and turbulent mixing in an Arctic shelf sea. *Elem Sci Anth* 5.

Wiles, P. J., Rippeth, T. P., Simpson, J. H., and Hendricks, P. J. (2006). A novel technique for measuring the rate of turbulent dissipation in the marine environment. *Geophysical Research Letters* 33. doi:10.1029/2006GL027050.

Woodgate, R. A., Weingartner, T. J., and Lindsay, R. (2012). Observed increases in Bering Strait oceanic fluxes from the Pacific to the Arctic from 2001 to 2011 and their impacts on the Arctic Ocean water column. *Geophysical Research Letters* 39. doi:10.1029/2012GL054092.

Zeitzschel, B., Diekmann, P., and Uhlmann, L. (1978). A new multisample sediment trap. *Marine Biology* 45, 285–288. doi:10.1007/BF00391814.